



Lead as an environmental toxicant in models of synucleinopathies

Liana Shvachiy^{a,b,c}, Ângela Amaro-Leal^{b,c,d}, Filipa Machado^b, Isabel Rocha^{b,c}, Vera Geraldes^{b,c,*}, Tiago F. Outeiro^{a,e,f,g,**}

^a University Medical Center Göttingen, Department of Experimental Neurodegeneration, Center for Biostructural Imaging of Neurodegeneration, Göttingen, 37073, Germany

^b Cardiovascular Centre of the University of Lisbon, Lisbon, 1649-028, Portugal

^c Institute of Physiology, Faculty of Medicine of the University of Lisbon, Portugal

^d Egas Moniz School of Health and Science, 2829-511, Caparica, Portugal

^e Max Planck Institute for Multidisciplinary Science, 37075, Göttingen, Germany

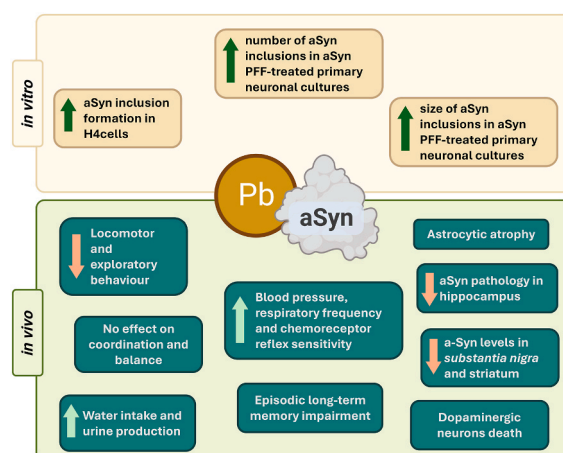
^f Translational and Clinical Research Institute, Faculty of Medical Sciences, Newcastle University, Framlington Place, Newcastle Upon Tyne, NE2 4HH, UK

^g Scientific Employee with an Honorary Contract at Deutsches Zentrum für Neurodegenerative Erkrankungen (DZNE), Göttingen, Germany

HIGHLIGHTS

- Lead exposure increases the number and size of alpha-synuclein (aSyn) inclusions in cell models.
- Animals exposed to aSyn fibrils and lead show increased phosphorylation of aSyn, neuronal damage and reduced astrogliosis in the *substantia nigra*.
- Lead-exposed animals exhibit impaired locomotion, anxiety, memory deficits, hypertension and chemoreceptor reflex hypersensitivity.
- The study suggests a mechanistic link between environmental lead exposure and the progression of diseases involving aSyn pathology, such as Parkinson's disease.

GRAPHICAL ABSTRACT



ARTICLE INFO

Handling editor: A. Gies

Keywords:

Alpha-synuclein
Parkinson's disease
Synucleinopathies

ABSTRACT

Lead, a toxic heavy metal, is prevalent in various industrial applications, contributing to environmental contamination and significant health concerns. Lead affects various body systems, especially the brain, causing long-lasting cognitive and behavioral changes. While most studies have focused on continuous lead exposure, intermittent exposure, such as that caused by migration or relocations, has received less attention. Importantly, lead exposure intensifies the severity of Parkinson's disease (PD) and dementia with Lewy bodies, diseases involving the accumulation of alpha-synuclein (aSyn) in the brain and in the gut. Although the precise

* Corresponding author. Instituto de Fisiologia, Faculdade de Medicina de Lisboa, Av Prof Egas Moniz, 1649-028 Lisbon, Portugal.

** Corresponding author. Department of Experimental Neurodegeneration, University Medical Center Göttingen, Göttingen, Waldweg 33, 37073, Göttingen, Germany.

E-mail addresses: vgeraldes@medicina.ulisboa.pt (V. Geraldes), tiago.outeiro@med.uni-goettingen.de (T.F. Outeiro).

<https://doi.org/10.1016/j.chemosphere.2025.144477>

Received 2 December 2024; Received in revised form 8 April 2025; Accepted 5 May 2025

Available online 9 May 2025

0045-6535/© 2025 The Authors. Published by Elsevier Ltd. This is an open access article under the CC BY license (<http://creativecommons.org/licenses/by/4.0/>).

Lead
Heavy-metal exposure
Environmental factor

mechanisms underlying these observations remain unclear, oxidative stress and mitochondrial dysfunction likely play a role. Here, we investigated how two different profiles of lead exposure - continuous and intermittent - affect models of synucleinopathies. We found that lead exposure enhances the formation of aSyn inclusions, resulting in an increase in both their number and size in cell models. In addition, we found that animals injected with aSyn pre-formed fibrils display serine 129-phosphorylated aSyn inclusions and a reduction in astrocytes in the substantia nigra. These animals also display neuronal damage and alterations in locomotor activity, exploration behavior, anxiety, memory impairments and hypertension. Our results suggest a mechanistic link between environmental lead exposure and the onset and progression of diseases associated with aSyn pathology. Understanding the molecular and cellular interactions between lead and aSyn is crucial for shaping public health policies and may provide novel insight into strategies for mitigating the impact of environmental toxins on neurodegenerative processes involved in Parkinson's disease and related synucleinopathies.

1. Introduction

Lead, a naturally occurring heavy metal (chemical element Pb), is used in a variety of widely used items such as automobiles, paints, and traditional cosmetics. Its broad usage has resulted in environmental damage, particularly contamination of drinking water, resulting in human exposure and, thereby, in public health consequences (Sani and Amanabo, 2021; Tempowski and World Health Organization, 2021; Wani et al., 2015; World Health Organization, 2021, 2010). Lead toxicity is a major environmental health concern, with the World Health Organization estimating a loss of around 1 million lives, in 2019, due to lead exposure (World Health Organization, 2021). There are two forms of lead exposure: (i) occupational or acute exposure and (ii) environmental or chronic exposure, with the latter being more dangerous in the long term (Organization, 2022; World Health Organization, 2010, 2021). Surprisingly, new environmental lead exposure profiles have been recently described, including the intermittent lead exposure profile that has been extensively studied and characterised in our laboratory in recent years, which has different health effects to those that have been extensively studied over several years (chronic/permanent lead exposure) (Liana Shvachiy et al., 2020; Shvachiy et al., 2018, 2022, 2023).

Lead is primarily found in soft tissues such as the brain, liver, and kidneys and accumulates in bones and teeth for long-term storage. In women, lead is released during pregnancy, exposing the foetus (Sani and Amanabo, 2021). Children are particularly vulnerable to lead toxicity as they absorb 4–5 times lead than adults (Academy et al., 2005; Laura Mayans, n.d.). The most serious consequences are a reduction in cognitive performance and behavioral problems in children (Academy et al., 2005; Koller et al., 2004). Adults may experience hematological consequences such as anemia, gastrointestinal disturbances such as stomach colic, and renal dysfunction (D. A. Gidlow, 2015; Flora et al., 2012; Todd et al., 1996; Wani et al., 2015). However, the major health impacts include cardiovascular dysfunction, an elevated risk of hypertension, ischemic heart disease, and stroke, along with neurological disturbances like headaches, irritability, depression, lethargy, convulsions, muscle weakness, ataxia, tremors, and hearing loss (Vaziri, 2008; Virgolini and Aschner, 2021). Other major health consequences of lead include neurotoxicity and, more particularly, neurodegeneration, as it has previously been linked to numerous neurodegenerative disorders such as Alzheimer's disease (AD), Amyotrophic lateral sclerosis, and Parkinson's disease (PD) (Bihaqi et al., 2018; Chin-Chan et al., 2015; Mason et al., 2014; Rocha and Trujillo, 2019; Toscano and Guilarte, 2005; Waseem et al., 2014; Wu et al., 2008).

PD is a complex, chronic, and progressive neurodegenerative illness characterized by typical motor symptoms such as resting tremor, stiffness, postural instability, and bradykinesia (Ogun, 2002; Radhakrishnan and Goyal, 2018; Spillantini and Goedert, 2000). However, non-motor symptoms such as hyposmia, postprandial and orthostatic hypotension, supine hypertension, REM sleep behavior disorder, constipation, baroreflex dysfunction, depression, and dementia are also prevalent in PD (Chen et al., 2020; Elfil et al., 2020; Fleming, 2011; Goldstein, 2013; Ogun, 2002; Radhakrishnan and Goyal, 2018; Scorza et al., 2018; Spillantini and Goedert, 2000). Several of these non-motor symptoms

arise early in the illness. However, the patient is diagnosed with PD only after the motor symptoms are evident (Braak et al., 2003; Hawkes et al., 2010).

PD belongs to a group of neurological disorders known as synucleinopathies that are characterized by the accumulation of intracellular protein inclusions rich in protein the alpha-synuclein (aSyn) (Coon and Singer, 2020; Goedert et al., 2017; Henderson et al., 2019; Murray et al., 2001). Although the precise biochemical function of aSyn is unclear, it is thought to regulate the pool and release of synaptic vesicles in neurons (Iwatsubo, 2007; Marques and Outeiro, 2012; Mehra et al., 2019; Wong and Krainc, 2017). Nevertheless, aSyn is not only a neuronal protein and is also present in other tissues such as the heart, muscles, and blood (He et al., 2021; Marques and Outeiro, 2012; Pinho et al., 2019a).

A link between lead exposure and PD has already been shown, most notably in studies that found that occupational exposure to lead increase the risk of PD (Coon et al., 2006; Gorell et al., 1997; Parsian et al., 2021; Paul et al., 2021; Weisskopf et al., 2010a). Relatively few studies have focused on the impact of lead on aSyn (Bihaqi et al., 2018; Zhu et al., 2011). However, to our knowledge, the effect of lead on aSyn aggregation in cell and animal models, and associated phenotypic alterations, have not been studied. Here, we conducted a detailed characterization of the effects of two different lead exposure profiles in models of aSyn pathology. Ultimately, our goal was to obtain insight into molecular and functional effects that can form the basis not only for informed preventive public health measures, but also for possible strategies for therapeutic intervention.

2. Methods

2.1. *In vitro* studies

2.1.1. Preparation of recombinant human aSyn protein species

The preparation of recombinant human aSyn protein was performed using an established protocol (Al-Azzani et al., 2022). Briefly, the plasmid pET21-aSyn encoding for human aSyn was transformed into competent *E. coli* BL21-DE3 (Sigma, Germany), and cells were grown in 2x LB medium (Sigma, Germany) with 200 g/mL ampicillin (Carl Roth, Germany) at 37 °C with shaking. The expression was induced for 2 h with 1 mM isopropyl-thiogalactopyranoside (IPTG, Apollo, UK) at OD600 0.5–0.6.

Before boiling for 15 min at 95 °C, lysates were sonicated on ice for 5 min (30s on, 30s off pulses, 60 % power). The supernatant containing aSyn was obtained after boiling the protein samples. Supernatants were purified using anion exchange chromatography (HiTrap Q HP, GE Healthcare) on Äkta Pure 25 M (Cytiva) with a mobile phase of 25 mM Tris pH 7.6 and a linear gradient of 9 column volumes of elution buffer to 1 M NaCl. Protein absorbance at 280 nm was measured, and aSyn concentration was calculated using the molar extinction coefficient 5960 M⁻¹cm⁻¹. To evaluate protein purity, 5 g of each sample was run on a 15 % SDS-PAGE gel and stained with Coomassie dye.

To generate seed fibrils (PFF), 200 μM of monomeric aSyn solution was incubated in a 96-well plate at 37 °C with 500 rpm shaking in the presence of Teflon polybeads. The fibrils were precipitated by

ultracentrifugation for 1.5 h at 15 °C in an Optima MAX-TL (Beckman Coulter, Fullerton, CA) with a TLA-120.2 rotor at 80,000 rpm. The supernatant was carefully removed after centrifugation, and the pellet was washed twice with PBS. The resulting pellet of amyloid fibrils was resuspended in PBS after 1 min of sonication in a bath-type ultrasonicator (Branson 1510, Danbury, CT). Before usage, the amyloid fibrils were kept at 4 °C and re-sonicated for 1 min.

2.2. Cell cultures and treatments

2.2.1. Primary neuronal cultures

C57BL6/J#00245 wild-type E15.5 mouse embryos, obtained from the University Medical Center Göttingen animal facility (Göttingen, Germany), were used to prepare primary whole brain neuronal cultures, as previously described (Caldeira Brás et al., n.d.). Pregnant animals were sedated with carbon dioxide poisoning and the embryos were removed from the uterus. Following meningeal excision, the whole brain was dissected under a stereomicroscope and transferred to ice-cold 1x Hanks' balanced salt solution (CaCl₂ and MgCl₂ free) (HBSS; Gibco Invitrogen, CA, USA) supplemented with 0.5 % sodium bicarbonate solution (Sigma-Aldrich, MO, USA). The process was halted by adding 100uL fetal bovine serum (FBS; Anprotec, Bruckberg, Germany) and 100 µL DNase I (0.5 mg/mL; Roche, Basel, Switzerland) after 15 min (min) of trypsinization (100 µL of 0.25 % trypsin; Gibco Invitrogen, CA, USA). After dissociation, the cell suspension was centrifuged at 300×g for 5 min before being resuspended in a pre-warmed neurobasal medium supplemented with 2 % B27 supplement (Gibco Invitrogen, CA, USA), 0.25 % GlutaMAX (Gibco Invitrogen, CA, USA), and 1 % penicillin-streptomycin (PAN Biotech, Aidenbach, Germany). For immunocytochemistry investigation, cells were seeded on coverslips covered with poly-L-ornithine (0.1 mg/mL in borate solution) (PLO; Sigma-Aldrich, MO, USA) in 24-well culture plates (Corning, Merck, Darmstadt, Germany) in a density of 150000 cells/well. The cells were maintained at 37 °C with 5 % CO₂, monitored closely and a new medium was added every 3–4 days.

2.2.2. Lead exposure and aSyn species treatment of primary neuronal cultures

Lead (II) acetate trihydrate (Sigma-Aldrich Chemie, Germany) was first diluted to 1 M concentration in bi-distilled water. The initial concentration was then diluted into several intermediate concentrations of 500 µM (0.5 mM), 1 mM, 5 mM and 10 mM solutions that were later added to the media of the primary neuronal cultures to dilute these into 1:1000 concentration to the final concentrations of 500 nM (0.5 µM), 1, 5, and 10 µM in the cultures. For permanent exposure, the intermediate lead solution was added on the day *in vitro* 5 (DIV5) and left in the neuronal culture until the day *in vitro* 21 (DIV21). For intermittent exposure, the intermediate lead solution was also added on the day *in vitro* 5 (DIV5), the lead solution was withdrawn on the day *in vitro* 7 (DIV7) by changing the media of the primary neuronal cultures and then added again on the day *in vitro* 14 (DIV14) until DIV21. The cells were closely monitored throughout the entire lead exposure time under the Whitefield microscope.

On day *in vitro* 7 (DIV7), after the media change in the cells, the cells were treated with 100 nM of the different aSyn species, namely Monomers and Preformed fibrils (PFFs). PBS was used as a vehicle and control of the treatment. For Monomers solution preparation, the aliquots were thawed in ice and centrifuged at 14000g at 4 °C for 25 min. The supernatant was taken out and diluted in sterile Dulbecco's phosphate-buffered saline (DPBS, PAN Biotech, Germany) and added to the cells to a final concentration of 100 nM. The PFFs were first thawed at room temperature, diluted in DPBS, and then sonicated for 1 min in the bath-type ultrasonicator (Branson 1510, Danbury, CT). The fibrils were then added to the cells at a final concentration of 100 nM.

2.2.3. H4 cell culture and transfection

Human neuroglioma cells (H4) were maintained in Opti-MEM I Reduced Serum Medium (Life Technologies- Gibco, Carlsbad CA, USA) supplemented with 10 % Foetal Bovine Serum Gold (FBS) (PAA, Cölbe, Germany) and 1 % Penicillin-Streptomycin (PAN, Aidenbach, Germany). The cells were grown at 37 °C with a 5 % CO₂ environment. Twenty-four hours prior to transfection, approximately 80000 H4 cells/well were plated in a 12-well plate (Costar, Corning, New York, USA) in 1 mL Optimem medium. Six hours prior to transfection medium was replaced with a fresh one.

Transfection was performed using FuGENE® HD Transfection Reagent, as described by the manufacturer. Briefly, the transfection reagent was removed from the 4 °C and left to get to room temperature. The vial of FuGENE® HD Transfection Reagent was vortexed until no precipitate was visible. In a 2 mL Eppendorf tube, FuGENE® HD Transfection Reagent was added directly in a specific calculated volume in Optimem medium without adds. The ratio of 1 (equal amounts of the plasmids encoding SynT with Synphilin-1-V5):3 (FuGENE® HD Transfection Reagent). The final prepared mix was calculated as 100uL to be added to the cells in the wells. For example, for 1 well, 1ug of SynT plasmid + 1ug Synphilin-1-V5 plasmid (total of 2ug) + 6uL of FuGENE® solution + 100uL Optimem without adds media was prepared. The mix was incubated for 30 min and added dropwise to the cells while the plate was gently rocked.

2.2.4. Lead exposure of H4 cells

As for the primary neuronal cultures, lead (II) acetate trihydrate (Sigma-Aldrich Chemie, Germany) was first diluted to 1 M concentration in bi-distilled water. This initial concentration was then diluted to the intermediate concentrations of 50 mM and 100 mM solutions that were used for the experiments in a 1:1000 dilution to final concentrations of 50 and 100uM in the cultures.

For permanent exposure, 24 h post-transfection, the lead solution was added and left on the plate for 24 h. For intermittent lead exposure, the cells were exposed to lead after 24 h of transfection, the lead was removed after 8 h of exposure (the medium was aspirated and new Optimem medium added) for 12 h and the lead was added again for another 4 h. A total of 24-h exposure protocol was applied in an intermittent paradigm.

2.3. Immunocytochemistry (ICC)

At the end of the lead exposure protocol, primary whole brain neuronal cultures and H4 cells were washed with 1x DPBS (PAN Biotech, Aidenbach, Germany) and fixed with 4 % of paraformaldehyde solution (PFA) for 20 min (home-made) at room temperature (RT). Cells were then washed 3 times with DPBS 1x solution (PAN Biotech, Aidenbach, Germany) and permeabilized with 0.1 % Triton X-100 (Sigma-Aldrich, MO, USA) for 10 min at RT, and then incubated with 3 % BSA in PBS (NZYTech) blocking solution for 1h at RT. Incubation with primary antibodies (1:1000) was performed overnight at 4 °C [primary neuronal cultures: MAP2 (mouse, ab11267, abcam), phosphorylated alpha synuclein S129 – paSyn S129 (rabbit, ab51253, abcam) and H4 cells: alpha synuclein (mouse, 610787, BD Biosciences)].

Subsequently, the cells were washed three times with PBS 1x solution (PAN Biotech, Aidenbach, Germany) and then incubated with fluorescence conjugated secondary antibodies (1:1000) for 2h at RT [primary neuronal cultures: Alexa Fluor 488 goat anti-rabbit (A11008, Invitrogen) and Alexa Fluor 568 goat anti-mouse (A-11004, ThermoFisher) and H4 cells: Alexa Fluor 488 goat anti-mouse (A11029, Invitrogen)]. Finally, cells were stained with DAPI (Carl Roth, Karlsruhe, Germany) (1:10000 in PBS 1x) for 10 min, and the coverslips mounted in SuperFrost® Microscope Slides treated with Mowiol (Calbiochem, San Diego, CA) dried and stored at room temperature until further visualization and analysis.

2.4. Imaging and analysis

Z-stack images of the primary neuronal cells were taken with a confocal point-scanning microscope (Zeiss LSM 900 with Airyscan 2, Carl Zeiss AG, Oberkochen, Germany) with a 10× objective (Objective Plan-Apochromat 10×/0.45 M27×) with tile scan, 20× objective (Objective Plan-Apochromat 20×/0.8×) and 63× objective (Objective Plan-Apochromat 63×/1.4 Oil DIC M27) for zoom in images of the neurons for fibril size analysis. For H4 cells, z-stack images were acquired in the same confocal microscope using the 63× objective with specific definitions for each staining.

Zen Microscopy Software (3.4 version, Carl Zeiss AG, Germany) was used for all the imaging experiments and the final images were post-analyzed and quantified using Fiji open-source software (Schindelin et al., 2012).

2.5. Primary neuronal cell image analysis

For quantification of the percentage of neuronal cells with PFFs (paSyn S129-positive cells), the 10x tile images were selected and a 3D object counter plugin in Fiji was used to first count the MAP2-stained neuronal cells and afterwards count the number of paSyn S129-positive cells. The following equation was applied for calculating the percentage of cells: (paSyn S129-positive cells/MAP2-positive neurons) × 100. To quantify the size of the fibrils, individual fibrils (paSyn S129-positive structures) were selected inside the cells and their area was measured using Measure analysis of Fiji in the 63x images. To represent that these fibrils are inside the neurons, we are showing the orthogonal projection images.

2.6. H4 cell image analysis

To quantify the number of aggregates and the size of the aggregates (area of the inclusions) inside the cells, the aSyn channel was selected and the images were thresholded. The images were then analyzed using the Analyze particle plugin from Fiji open-source software.

2.7. In vivo studies

2.7.1. Lead exposure animal model

The lead exposure models were developed as described previously (Geraldés et al., 2016; Guimarães et al., 2012). Seven-day-pregnant Wistar rats (Charles River Laboratories, Chatillon-sur-Chalaronne, France) were separated into Pb-treated and control groups. The tap drinking water in the Pb-treated group was replaced with a 0.2 % (p/v) lead (II) acetate solution (Acros Organics, New Jersey, NJ, USA) dissolved in deionized water.

The pups, after weaning at 21 days, were divided into 6 groups according to the type of exposure and brain injection. The 0.2 % lead acetate solution was given to the lead exposed groups: intermittent groups (IntPb, n = 48) – lead exposure until 12 weeks of age, no exposure (tap water) until 20 weeks, and second exposure from 20 to 28 weeks of age; permanent groups (PerPb, n = 42) – lead solution in the animal diet until 28 weeks of age. Tap water was given to the age-matched control groups (Ctrl, n = 38).

To offer a full functional and morphological evaluation, all animals were exposed to the same experimental methodology. The experimental methodology complied with European and national animal welfare regulations and was authorized by the Academic Medical Centre of Lisbon, Portugal (ref. 411/16). A timeline with lead exposure animal model and all methodologies is shown in Fig. 1.

2.8. Intrastratial stereotaxic injections

Immediately before injection, recombinant aSyn PFF from the same batch as used for the *in vitro* studies, were thawed, diluted in sterile PBS solution, and sonicated for 1 min in a bath-type ultrasonicator (Branson, Danbury, CT). Animals of 12 weeks (3 months) of age were anaesthetized with a mixture of Ketamine/Dexmedetomidine, 0.2 ml/100g in weight, administered intraperitoneally and the withdrawal reflex was checked. Temperature was maintained through a homoeothermic blanket (Harvard Apparatus, Cambourne, UK). When the withdrawal was not present, the animals were placed into a stereotaxic device (Kopf Instruments, Tujunga, CA, USA) and the head of the animal was fixed

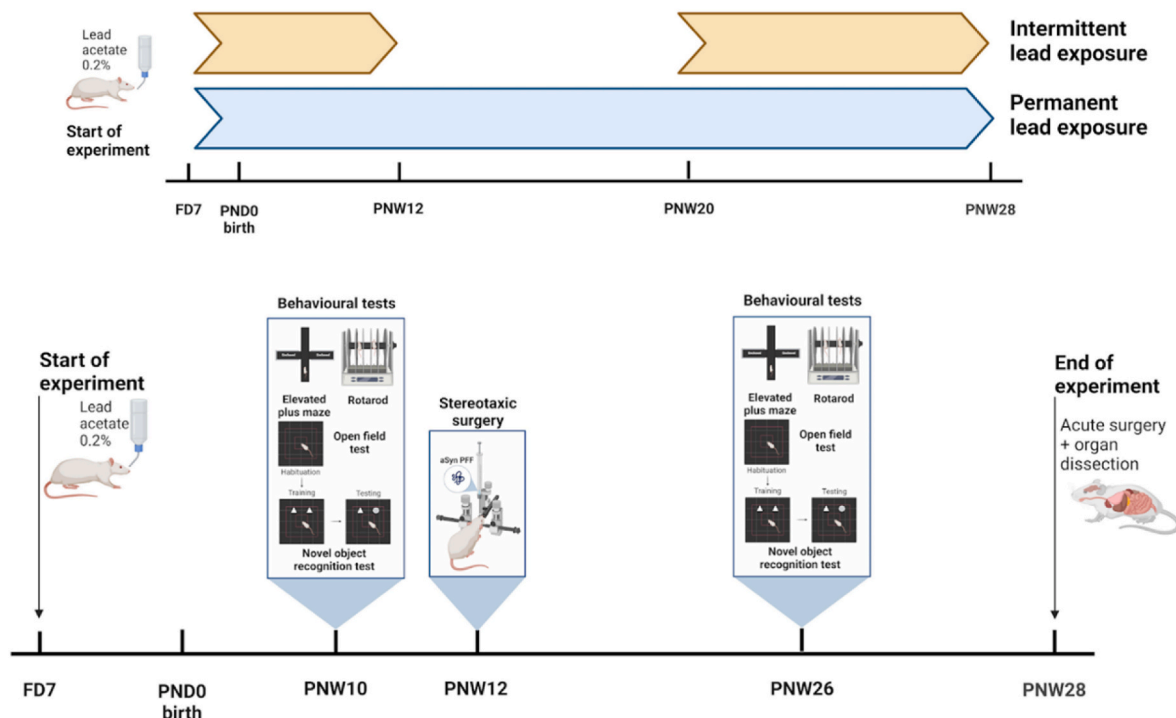


Fig. 1. Experimental timeline of lead exposure animal model and experimental protocol.

with ear bars from the device. Recombinant aSyn PFF solution or sterile PBS was injected into the right striatum at one site (8 µg protein; AP +1.6, ML +2.4, DV−4.2 from the skull) at a rate of 0.5 µl per minute using a microinjection pump (World Precision Instruments, Inc., Florida, USA). After each injection, the needle (10 µL, 33-gauge Hamilton micro syringe (Hamilton Company, Nevada, USA)) was left in place for 2 min and then slowly withdrawn. For control rats, the same volume of vehicle solution (PBS) was injected. The skin of the rat was sutured with Silkam® 4/0 silk sutures (B-Braun, Melsungen, Germany) after the syringe was removed, and Bepanthen® Plus (Bayer, Leverkusen, Germany) was put on top of the sutures. Individual animals were kept in recovery cages with heating pads until they regained ambulatory ability. At the end of the stereotaxic surgery protocol, the animals were divided into 6 experimental groups according to the lead exposure and type of injection: Ctrl PBS, Ctrl aSyn; IntPb PBS, IntPb aSyn, PerPb PBS and PerPb aSyn.

2.9. Behavioral evaluation

The animals were subjected to a battery of standard behavioral tests two weeks prior to the functional evaluation (at 26 weeks of age). Behavioral evaluations were performed to assess (i) motor function and coordination with rotarod (Creed and Goldberg, 2018; Deacon, 2013; Laurent et al., 2016), (ii) anxiety-like behavior using elevated plus maze (Naolapo et al., 2012), (iii) locomotor and exploratory behavior with open field test (Santos Alves et al., 2014), and (iv) episodic long-term memory via novel object recognition test (Antunes and Biala, 2012). During the experimental days, animals were kept in the behavior testing room for at least an hour before the testing session began.

All behavioral experiments were conducted between the hours of 8 a.m. and 6 p.m. in a quiet room with low lighting, and all animals went through a four-day handling period (Costa et al., 2012; Schmitt and Hiemke, 1998) for researcher and testing room habituation and bias reduction. Between animals, all behavioral equipment was cleaned with 70 % ethanol. All tests were videotaped using a UV camera (Chacon, Wavre, Belgium), and the movies were analyzed using ANY-maze software (Stoelting Co., Wood Dale, IL, USA).

2.10. Rotarod test

Motor function and coordination were tested on an accelerating rotarod (MED Associates Inc., St Albans, VT, USA) using the protocol described elsewhere (Creed and Goldberg, 2018; Deacon, 2013; Laurent et al., 2016; Lubrich et al., 2022). Rats were put on the rod with their heads pointing in the opposite direction of the rotation, forcing the animal to go forward to retain its equilibrium. Rats were first trained at a steady pace (7 r.p.m. for 5 min) before beginning three test trials (at least 30 min intertrial interval). Animals had to balance on a revolving rod that accelerated from 4 to 40 r.p.m. in 5 min during these trials. The time it took for the rats to fall off the revolving rod was timed to a maximum of 5 min and the r.p.m was also calculated.

2.11. Open-field exploration test

Taking advantage of the curious nature of the rodents, the open field test (OFT) was used for exploration of a new environment and general locomotion (Buccafusco, 2001). The OFT apparatus is composed of a square black box (67 x 67 x 57 cm in height) that has been "virtually" split into three concentric squares: (1) the periphery zone (near the walls), (2) the intermediate zone, and (3) the center. The animals were left in the maze to explore freely for 5 min, which is generally enough time to assess the specified parameters. We computed the total travelled distance and the average velocity of the animals as the main parameters of the test (Moreira et al., 2001; Ramos, 2008; Santos Alves et al., 2014; L. Shvachiy et al., 2020; Shvachiy et al., 2018).

2.12. Novel object recognition test

Novel object recognition test (NOR) with a 24-h retention interval was used to evaluate the episodic long-term memory by the same protocol as described previously using the OFT arena (Antunes and Biala, 2012; L. Shvachiy et al., 2020; Shvachiy et al., 2022, 2018). Briefly, the objects used (clear and brown glass shapes) were randomized and their position in relation to the other objects was changed to use each object as a source of familiarity or novelty.

The test consists of three stages: habituation, training, and testing. During habituation (three days), animals were left to explore the apparatus freely for 15 min. On the fourth day, they were exposed to two familiar (F) items, for 5 min. On the fifth day, the animals were exposed to two objects for 5 min, one previously encountered object (F) and one novel object (N) (Antunes and Biala, 2012). The testing day was recorded and analyzed using ANY-maze® software employing 3-point analysis (head, torso, and tail of the animal), and only the data from the head point analysis were relevant for object exploration. The amount of time animals spent around each object during the testing stage was used to quantify exploratory behavior. The number of approaches that involved smelling, rearing towards, or touching the item was tallied. Exploration did not include sitting rearward to the item or passing in front of it without pointing the nose in the object's direction (Antunes and Biala, 2012). Exploration time was measured as follows: $ET (\%) = (\text{time exploring the object} / \text{overall exploring time}) \times 100$.

The novelty index was computed as follows:

$$(\text{ET\% Novel} - \text{ET\% Sample}) / (\text{ET\% Novel} + \text{ET\% Sample}).$$

This index has a range of −1 to 1, with negative values representing the lack of discrimination between the new and familiar items (i.e., spending more time exploring the sample object or equal time exploring both items) and positive values representing more exploration of the novel object (Mouro et al., 2017; L. Shvachiy et al., 2020; Shvachiy et al., 2018).

2.13. Metabolic evaluation

Rats were housed in metabolic cages for 24 h before the acute experiment at 28 weeks to examine body weight, food and drink consumption, and urine and feces production.

2.14. Functional evaluation

2.14.1. Physiological and autonomic evaluation

After behavioral and metabolic evaluation, animals were anaesthetized with sodium pentobarbital (60 mg/kg, intraperitoneal injection). Anesthesia levels were maintained using a 20 % solution (v/v) of the same anesthetic after assessing the withdrawal response. A homeothermic blanket (Harvard Apparatus, Cambridge, UK) was used to keep the animal's temperature stable. To measure tracheal pressure, the trachea was cannulated below the larynx. The femoral artery and vein were cannulated to monitor blood pressure (BP) and inject saline and drugs, respectively. The electrocardiogram (ECG) was assessed using subcutaneous electrodes in three limbs, and the heart rate was calculated using the ECG data (Neurology, Digitimer, Welwyn Garden City, UK).

The right carotid artery was catheterized, and chemoreceptors were stimulated with lobeline (0.2 mL, 25 g/mL, Sigma, St. Louis, MO, USA) (Gerald et al., 2016). Phenylephrine injection (0.2 mL, 25 g/mL, Sigma, St. Louis, MO, USA) in the femoral vein was used to stimulate the baroreflexes (Gerald et al., 2016; L. Shvachiy et al., 2020; Shvachiy et al., 2018).

Blood lead levels (BLL) were determined from the venous blood using an atomic absorption spectrophotometer (Shimadzu, Model no. AA 7000, Kyoto, Japan). At the end of the above-mentioned acute experience, the animal was sacrificed with an overdose of anesthetic.

2.14.2. Data acquisition and analysis

Continuous recordings of blood pressure (BP), ECG, heart rate (HR), and respiratory frequency (RF) were performed (PowerLab, ADInstruments, Colorado Springs, CO, USA) and acquired, amplified, and filtered at 1 kHz (Neurology, Digitimer, Welwyn Garden City, UK; PowerLab, ADInstruments, Colorado Springs, CO, USA). A baseline recording of 10 min was taken for basal autonomic assessment. Each stimulus was separated by at least 3 min.

2.14.3. Baro- and chemoreceptor reflex analysis

The autonomic reflexes analysis was focused on assessing baro- and chemoreceptor responses. The baroreceptor reflex gain (BRG) was calculated after phenylephrine provocation by measuring $\Delta HR/\Delta BP$ (bpm/mmHg).

The chemoreflex response was estimated using respiratory frequency (RF) measured from tracheal pressure before and after lobeline stimulation: $\Delta RF = RF_{stimulation} - RF_{basal}$.

2.15. Immunohistochemistry (IHC)

After sacrifice, animals underwent transcardial perfusion with fresh PBS 1x solution (TH Geyer, Germany), the brain was removed and transferred into paraformaldehyde (PFA 4 %, Carl Roth, Germany) solution for post-fixation for 72h. The brains were then immersed in increasing concentrations of sucrose (15 % and 30 %, Merck, Germany in PBS 1x with sodium azide, Sigma, Germany) and kept at 4 °C for later analysis.

To evaluate the astrocytic, alpha-synuclein, phosphorylated alpha-synuclein and dopaminergic neurons changes, sagittal free-floating sections (30 μ m) were cut around the region of hippocampus [Lateral 0.6–2.04 using a cryostat (Leica CM 3050S, Germany)] and, subsequently stained as reported previously (Chegão et al., n.d.; Shvachiy et al., 2022). Succinctly, free-floating sections were washed with TBS 1x (PanReac/AppliChem, Germany), permeabilized with 3 % Triton X 100 solution for 15min (Carl Roth, Germany) and blocked with 5 % Goat Serum (BioWest, France) and 1 % Bovine serum (VWR, USA) for 1 h. The freely floating tissue were then incubated with specific combinations of primary antibodies [astrocytes - glial fibrillary acidic protein - GFAP (chicken, ab4674, abcam, 1:500), alpha synuclein (mouse, 610787, BD Biosciences), phosphorylated alpha synuclein S129 – paSyn S129 (rabbit, SMC-600, StressMarq), Tyrosine Hydroxylase - TH (mouse, MAB5280, Milipore) and Tyrosine Hydroxylase – TH (rabbit, AB152, Milipore)] overnight at 4 °C on a shaker.

Sections were then washed with TBS 1x and incubated with specific combinations of secondary antibodies [Alexa Fluor 488 donkey anti-mouse (A21202, ThermoFisher), Alexa Fluor 568 goat anti-rabbit (A11036, Invitrogen), Alexa Fluor 633 goat anti-chicken (A21103, Invitrogen), Alexa fluor 488 donkey anti-rabbit (A21206, Invitrogen) and Alexa Fluor 568 goat anti-mouse (A-11004, ThermoFisher)]. Lastly, nuclei were counter-stained with DAPI (4',6-diamidino-2-phenylindole, 1:10000, Carl Roth, Germany). Sections were mounted in SuperFrost® Microscope Slides using Fluoromount-G mounting media (Invitrogen, Germany). Omission of the primary antibody resulted in no staining.

Z-stack images of the dentate gyrus region of the hippocampus, striatum and *substantia nigra* were taken with a confocal point-scanning microscope (Zeiss LSM 900 with Airyscan 2, Carl Zeiss AG, Oberkochen, Germany) with a 20 \times objective (Objective Plan-Apochromat 20 \times /0.8 \times) and tile scan to image the specific region of interest and 63 \times objective (Objective Plan-Apochromat 63 \times /1.4 Oil DIC M27) for zoom in images of the cells for morphological evaluation of the astrocytic cells. Zen Microscopy Software (3.4 version, Carl Zeiss AG, Germany) was used for all the imaging experiments and the final images were post-analyzed and quantified using Fiji open-source software (Schindelin et al., 2012).

For morphological evaluation of the astrocytes, relevant scientific articles were used for support (Hol and Pekny, 2015; Siracusa et al., 2019; Sofroniew and Vinters, 2010). For quantification of the

percentage of GFAP-positive cells, the dentate gyrus region of the 20 \times tile images was selected and a 3D object counter plugin in Fiji was used to first count the DAPI-stained nuclei and afterwards count the number of GFAP-positive cells. The following equation was applied for calculating the percentage of cells: (GFAP-positive cells/DAPI nuclei) \times 100. Fluorescence intensity inside the cells and their area were measured using Measure analysis of Fiji in the 63 \times images with cells individually selected for analysis. For evaluation of the fluorescence intensity, the selected region of the dentate gyrus and the *substantia nigra* and the whole image of the striatum, the images were measured with the measure analysis from Fiji open-source software.

2.16. Statistical analysis

If not otherwise specified, the data were presented as mean \pm SD and represented the average of mean values across all animals/cells/biological repetitions. The normality distribution of continuous variables was assessed using the D'Agostino and Pearson normality test, and the homogeneity of variance was examined using Levene's test. For data analysis among different groups, in *in vitro* a one-way ANOVA was employed and *in vivo* studies encompassing behavioral, physiological, and molecular parameters, a two-way ANOVA was applied. Subsequently Tukey's multiple comparisons test was applied for normally distributed data, and Kruskal-Wallis multiple comparison test for non-normally distributed values. Additionally, to compare the exploration time percentage between objects in the NOR test for each group, a student t-test for paired observations was used. The statistical analysis was performed using GraphPad Prism 9 (GraphPad Software Inc., USA). Statistical significance was defined as $p < 0.05$.

3. Results

3.1. Lead exposure increases aSyn inclusion formation in H4 cells

First, to study the effect of lead exposure on aSyn inclusion formation, we used an established model of aggregation based on the co-expression of a modified form of aSyn (SynT) and synphilin-1 (Lázaro et al., 2017; McLean et al., 2001). Interestingly, we found that both types of lead treatment profiles induced an increase in the number of inclusions per cell (Fig. 2A–B) but not in the average size of the inclusions (Fig. 2C).

3.2. Lead exposure increases the number and size of inclusions in aSyn PFF-treated primary neuronal cultures

In order to assess the effect of lead in a neuronal cell model, we investigated the effect of lead in the generation of inclusion in primary neuronal cultures by the addition of pre-formed fibrils (PFFs). First, we confirmed the formation of inclusions in the cells by the addition of the different aSyn species, namely monomers and PFFs. As a control, we used the DPBS solution, being that the vehicle of the preparation of the species.

The orthogonal projections of the representative images of paSyn S129 staining for aggregates and MAP2 marker for neurons show that the PFFs treatment generated abundant aggregate formations in the cells in all groups. The orthogonal projection shows that these formations are inside the neurons (the green staining – paSyn S129 is enclosed in the red staining – MAP2, as observed in Fig. 3A) Curiously, we observed that neither PBS nor Mon lead to the formation of inclusions in the primary neuronal cells. Interestingly, we detected that the aggregates formed in the PFFs groups increase in number with the presence of lead with both intermittent and permanent lead exposure, with a significant increase in the percentage of neurons with inclusion in the PerPb 5 μ M group (Fig. 3C).

To evaluate the effect of lead on the size of aggregates in primary neurons, confocal images were taken and analyzed. Lead exposure

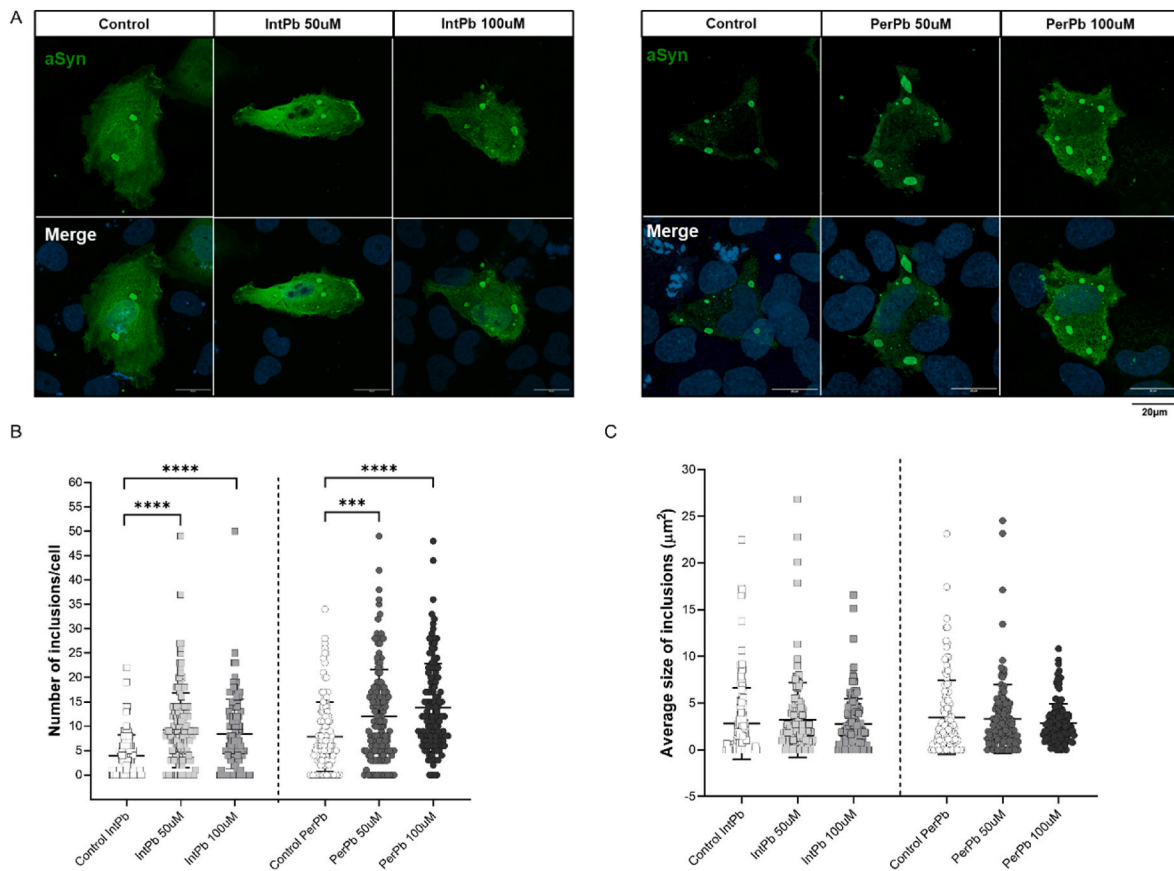


Fig. 2. Effect of lead on aSyn inclusion formation in H4 cells. A. Representative images of cells treated with lead and immunostained with an antibody against aSyn. B. Quantification of aSyn-positive inclusions inside the cells. C. Histogram of the average size of the inclusions. Images were acquired using a confocal point scanning microscope (Zeiss LSM 900 with Airyscan2) with a $63\times$ objective. Scale bar is $20\ \mu\text{m}$. Values are the mean \pm SD ($n = 123\text{--}163$ cells) with 3 independent experiments for each evaluated group. Symbols refer to statistically significant differences inter groups (Ctrl vs IntPb/PerPb - * $p < 0.05$, ** $p < 0.01$, *** $p < 0.001$, **** $p < 0.0001$); one-way ANOVA, Kruskal-Wallis multiple comparison test for non-normal values.

caused an increase in the size of the aggregates inside the cells (Fig. 3 B). Likewise, the neuronal cells from IntPb 1 and $5\ \mu\text{M}$ and PerPb 1 and $5\ \mu\text{M}$ appear to be in stronger distress as the cells show axonal damage (intermittent MAP2 signal), decreased growth of the dendrites and death of the cell body. The quantifications of the images showed that lead exposure, regardless of the type, causes an increase in the size of the inclusions. However, only the IntPb $1\ \mu\text{M}$ from the intermittent groups shows a significant increase. The IntPb 0.5 and $5\ \mu\text{M}$ groups did not cause a significant increase in the size of the aSyn inclusions. As for the permanent exposure groups, all PerPb groups show a significant increase in the size of the inclusions (Fig. 3 D).

3.3. Lead causes locomotor and exploration impairment in the aSyn PFF model without effect in coordination and balance

Next, to assess the effect of lead or aSyn PFF on motor performance of Wistar rats, we used the rotarod test. We observed no significant changes between the groups, regardless of the type of lead exposure or the injection, in the time spent on the rotarod (Fig. 4A). Therefore, no significant differences were observed in the rotations per minute (Fig. 4B).

To evaluate the locomotor and exploratory behavior of the animals, the open field test was used. A significant decrease in total travelled distance was observed in PerPb PBS when compared to Ctrl PBS and when compared to Ctrl aSyn, and in both IntPb aSyn and PerPb aSyn when compared to Ctrl aSyn and to Ctrl PBS with significant changes between IntPb PBS with other groups (Fig. 4C).

A similar pattern of changes was observed in the average velocity. Namely, a significant decrease was observed in the PerPb PBS compared

to Ctrl PBS and Ctrl aSyn as well as IntPb aSyn and PerPb aSyn showed a significant decrease when compared to Ctrl aSyn and Ctrl PBS without significant differences between IntPb PBS and other groups (Fig. 4D).

3.4. Lead impairs episodic long-term memory alongside aSyn PFF injection

Next, we used the novel object recognition test to evaluate effects in episodic long-term memory with a retention interval of 24 h. Regarding the exploration time, we observed that only the Ctrl PBS group shows a significant reduction in this parameter (Fig. 5A). No significant changes were observed in the other groups (Fig. 5A). Interestingly, when the novelty recognition index was calculated, we observed that both lead exposed groups, without aSyn, showed a significant decrease in this parameter (Fig. 5B). Interestingly, no aSyn group (Ctrl, IntPb or PerPb) showed significant differences when compared to the other groups (Fig. 5B).

3.5. Lead increases blood pressure, respiratory frequency and chemoreceptor reflex sensitivity

During the acute surgery at 28 weeks of age, basal physiological parameters were evaluated 10 min before the stimulations of the autonomic reflexes. We observed that, regardless of the lead exposure and/or injection of aSyn, the animals showed a significant increase in the systolic, diastolic and, consequently, mean blood pressure, when compared to the Ctrl PBS group (Fig. 6A), but no changes in heart rate (Fig. 6B). A significant increase was observed in the respiratory frequency in the

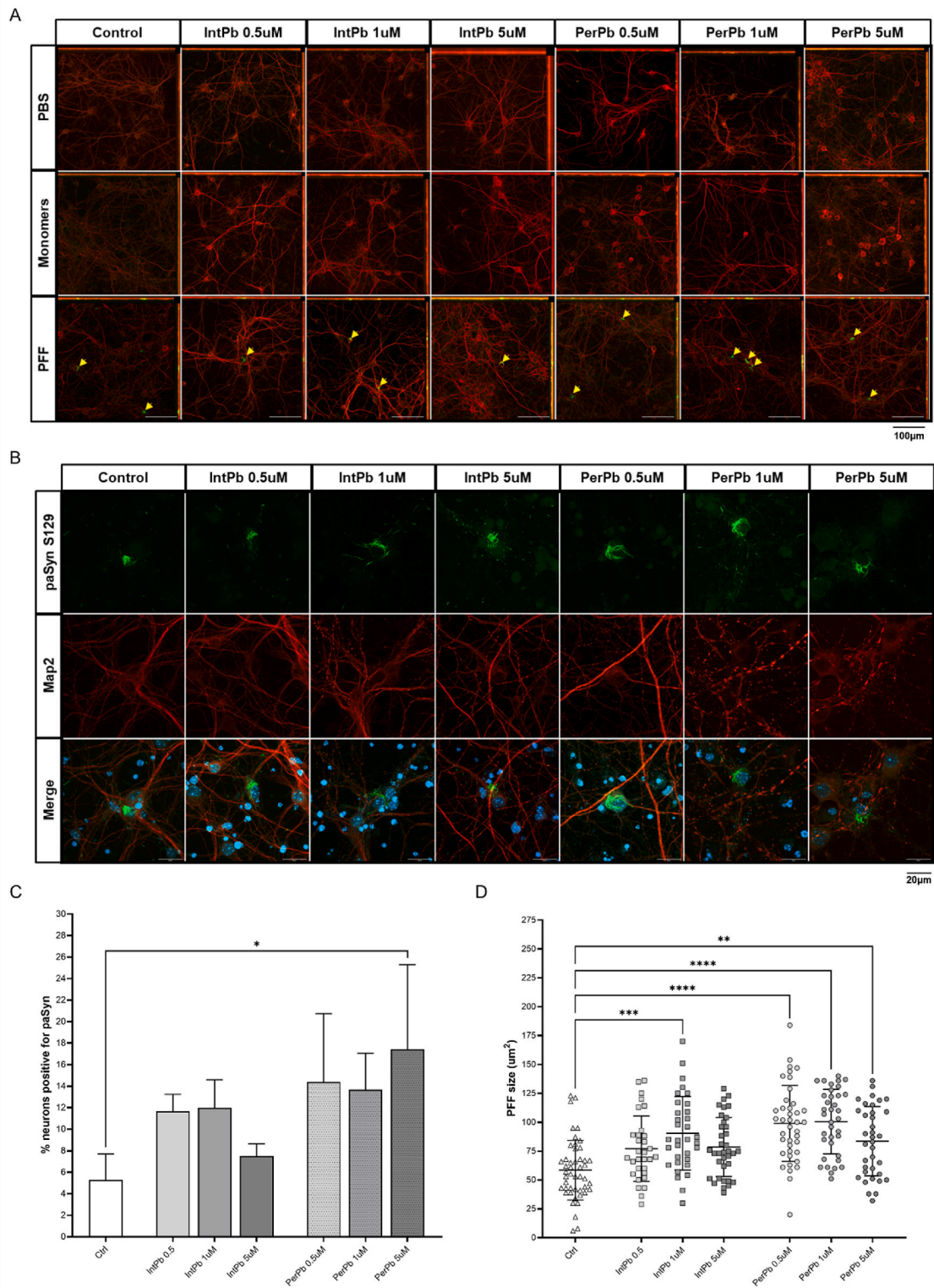


Fig. 3. Effect of lead exposure on aSyn aggregation in primary neuronal culture. A. Representative images of the orthogonal projection images of neuronal cells treated with the different aSyn species, stained with paSyn antibody (1:1000), exposed to lead and controls. B. Representative images of the 63× magnification images of neuronal cells treated with the different aSyn species, stained with paSyn antibody (1:1000), exposed to lead and controls. C. Histogram of the quantification of the number of neurons with paSyn-stained aggregates inside the cells of 10× magnification images; $F = 3.771$. D. Histogram of the quantification of the size of the paSyn-stained aggregates inside the neurons; $F = 10.56$. Images were acquired using a confocal point scanning microscope (Zeiss LSM 900 with Airyscan2) with 10x, 20x and 63× objectives. Scale bar is 100 µm and 20 µm for representative images. Nomenclature: IntPb – Intermittent lead exposure with different concentrations (0.5, 1, 5uM); PerPb – Permanent lead exposure in different concentrations (0.5, 1, 5uM). Values are the mean ± SD ($n = 3-5$ independent experiments for each evaluated group and $n = 31-47$ cells). The symbols denote statistically significant differences inter groups (Ctrl vs IntPb/PerPb - * $p < 0.05$, ** $p < 0.01$, *** $p < 0.001$, **** $p < 0.0001$); one-way ANOVA, Tukey's multiple comparison test and Kruskal-Wallis multiple comparison test for non-normal values.

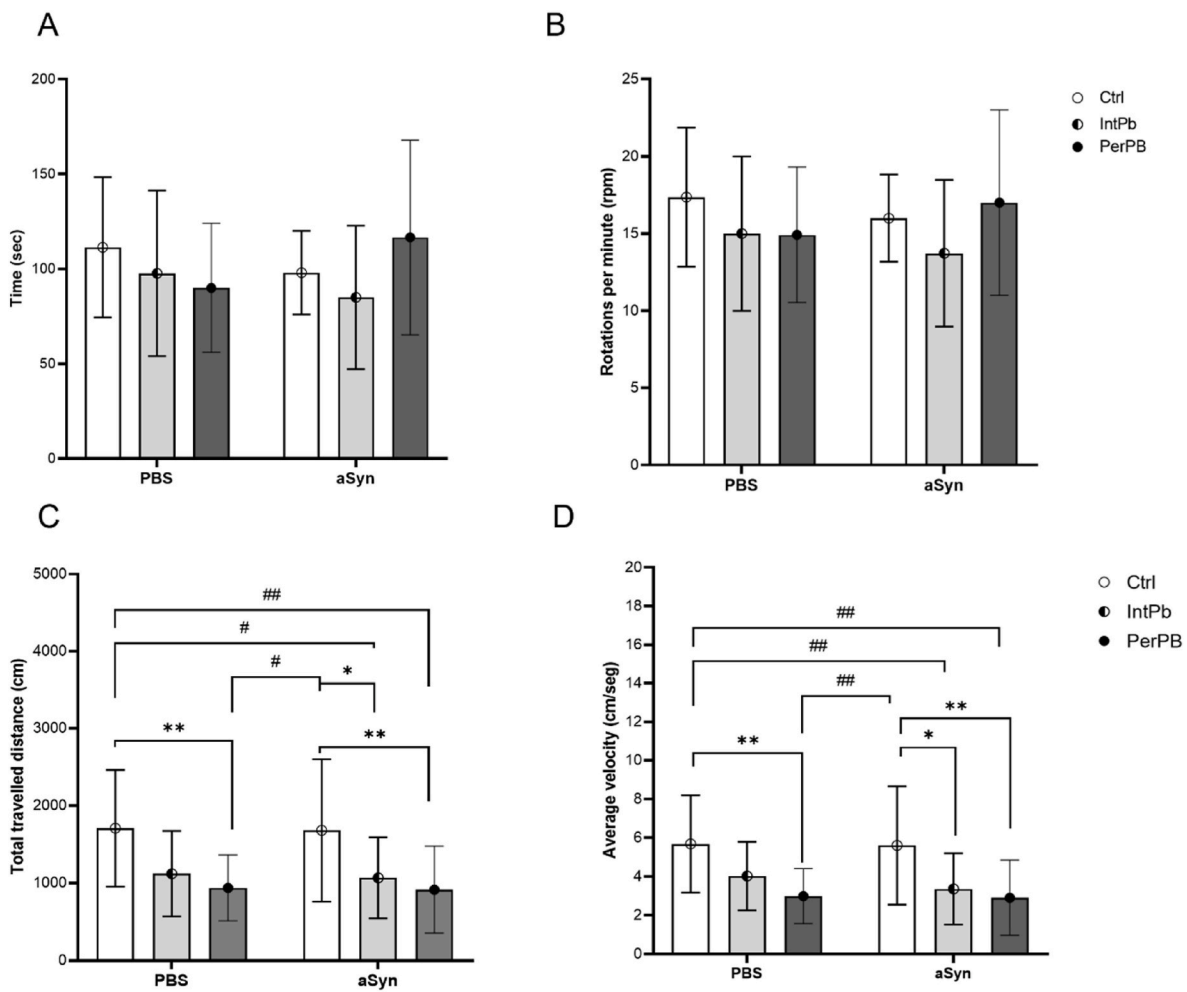


Fig. 4. Effect of lead exposure and aSyn PFF injection in the motor coordination balance, locomotor and exploratory behaviour. A. Time spent in the rotarod apparatus or latency to fall; $F(2,72) = 2.190, p = 0.1193$. B. Rotations per minute on the rotarod apparatus; $F(2,74) = 1.116, p = 0.3332$. C. Total travelled distance in the open field test; $F(2,107) = 0.0067, p = 0.9932$. D. Average velocity in the open field test; $F(2,110) = 0.253, p = 0.7769$. Values are the mean \pm SD. The symbols denote statistically significant differences inter groups: Ctrl PBS vs IntPb PBS/PerPb PBS; Ctrl aSyn vs IntPb aSyn/PerPb aSyn - * $p < 0.05$, ** $p < 0.01$, *** $p < 0.001$, **** $p < 0.0001$; Ctrl PBS vs IntPb aSyn/PerPb aSyn; two-way ANOVA, Tukey's multiple comparison test.

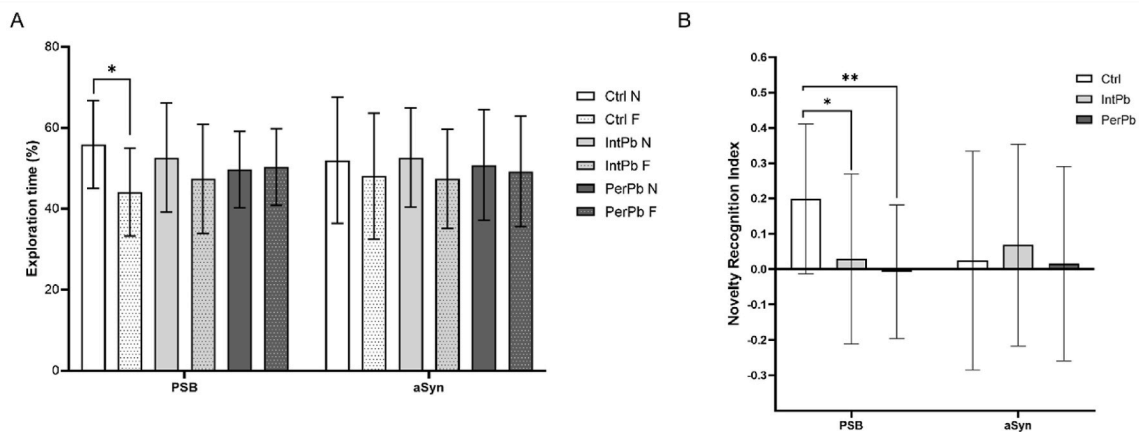


Fig. 5. Effect of lead exposure and aSyn PFF injection in episodic long-term memory. A. Exploration time percentage of novel (N) and familiar (F) objects; $F(5,308) = 0.4563, p = 0.8086$. B. Novelty recognition index was calculated; $F(2,143) = 2.72, p = 0.0689$. Values are the mean \pm SD. The symbols denote statistically significant differences inter groups: Ctrl PBS vs IntPb PBS/PerPb PBS; Ctrl aSyn vs IntPb aSyn/PerPb aSyn - * $p < 0.05$, ** $p < 0.01$, *** $p < 0.001$, **** $p < 0.0001$; Ctrl PBS vs IntPb aSyn/PerPb aSyn; Ctrl aSyn vs IntPb PBS/PerPb PBS - # $p < 0.05$, ## $p < 0.01$, ### $p < 0.001$, #### $p < 0.0001$; Ctrl PBS vs Ctrl aSyn/IntPb PBS vs IntPb aSyn/PerPb PBS vs PerPb aSyn - * $p < 0.05$, ** $p < 0.01$, *** $p < 0.001$, **** $p < 0.0001$; two-way ANOVA, Tukey's multiple comparison test; the differences between the objects (N and F) in the exploration time percentage was analyzed with Paired t -test.

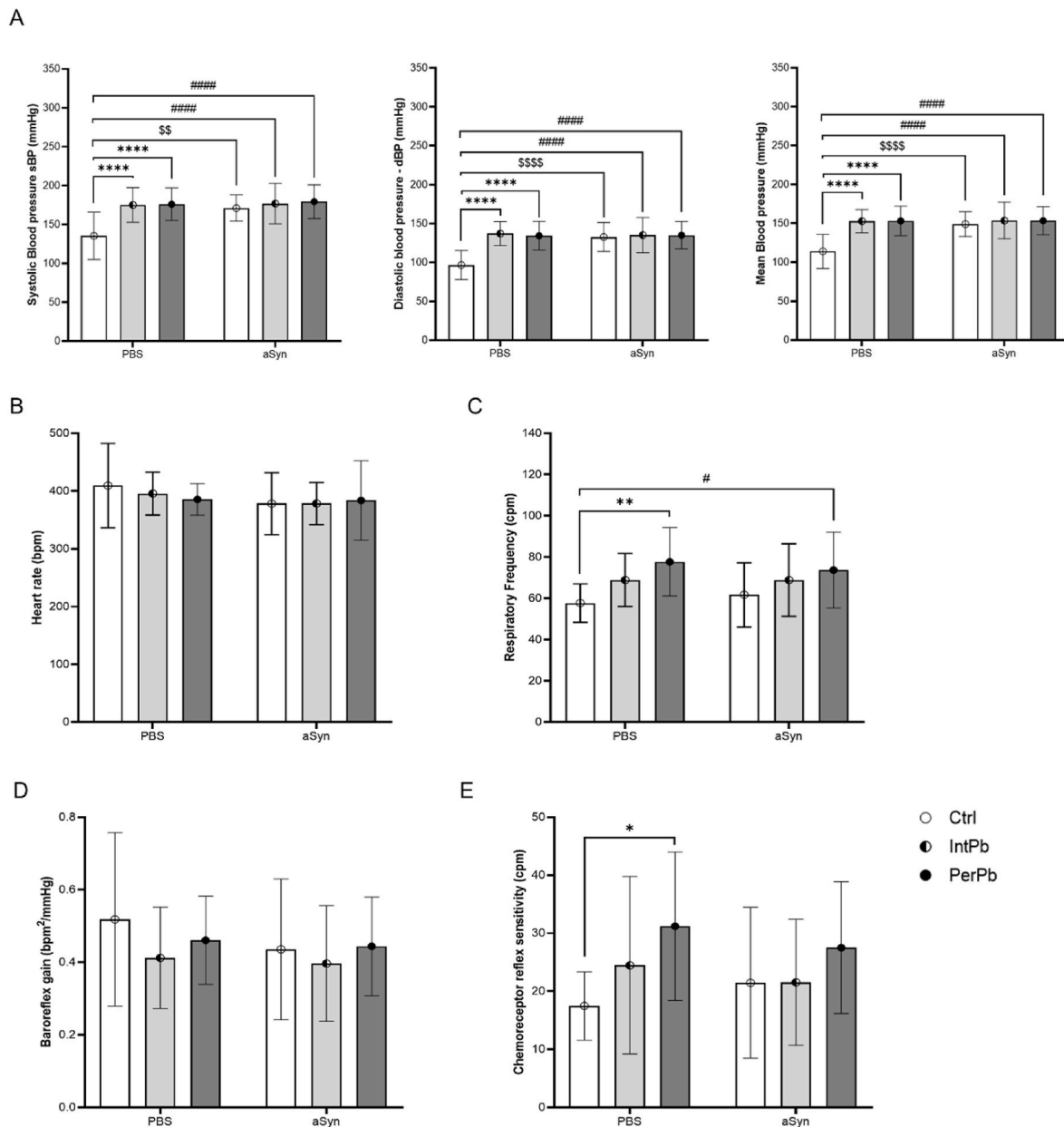


Fig. 6. Effect of lead exposure and aSyn PFF injection in basal physiological parameter and autonomic reflexes. A. Systolic, diastolic, and mean blood pressure; sBP - $F(2,102) = 5.23$, $p = 0.0069$, dBP $F(2,102) = 9.929$, $p = 0.0001$, mBP - $F(2,102) = 8.24$, $p = 0.0005$. B. Heart rate; $F(2,102) = 0.7005$, $p = 0.4987$. C. Respiratory frequency; $F(2,100) = 0.5242$, $p = 0.5937$. D. Baroreflex gain; $F(2,96) = 0.4103$, $p = 0.6646$. E. Chemoreceptor reflex sensitivity; $F(2,99) = 0.8462$, $p = 0.4321$. Values are the mean \pm SD. The symbols denote statistically significant differences inter groups: Ctrl PBS vs IntPb PBS/PerPb PBS; Ctrl aSyn vs IntPb aSyn/PerPb aSyn - * $p < 0.05$, ** $p < 0.01$, *** $p < 0.001$, **** $p < 0.0001$; Ctrl PBS vs IntPb aSyn/PerPb aSyn; Ctrl aSyn vs IntPb PBS/PerPb PBS - # $p < 0.05$, ## $p < 0.01$, ### $p < 0.001$, #### $p < 0.0001$; Ctrl PBS vs Ctrl aSyn/IntPb PBS vs IntPb aSyn/PerPb PBS vs PerPb aSyn - \$ $p < 0.05$, \$\$ $p < 0.01$, \$\$\$ $p < 0.001$, \$\$\$\$ $p < 0.0001$; two-way ANOVA, Tukey's multiple comparison test.

permanently lead-exposed animals, independently of aSyn injection, when compared to the Ctrl PBS group with no other significant changes in other groups (Fig. 6C).

After evaluating the basal physiological parameters, the autonomic reflexes were pharmacologically stimulated. We observed that, even though there is a slight decrease in the baroreflex gain, no significant differences were present in all the groups, regardless of lead exposure or injection (Fig. 6D). Interestingly, only the PerPb PBS group, showed a significant increase in the chemoreceptor reflex sensitivity, when compared to the Ctrl PBS group with no other significant changes in this parameter (Fig. 6E).

3.6. Lead increases blood lead levels (BLL), water intake and urine production in a model of aSyn pathology

The metabolic evaluation was performed for 24 h in metabolic cages after the behavioral testing at 28 weeks of age. We observed that the intermittent lead exposure group injected with aSyn (IntPb aSyn) animals had a strong decrease in the water intake when compared to both Ctrl aSyn and Ctrl PBS groups. Interestingly, the IntPb PBS and PerPb PBS groups showed a significant decrease in urine production when compared to the Ctrl aSyn group. The IntPb aSyn group, similarly to the water intake, showed a significant decrease in urine production when compared to the Ctrl aSyn group (Fig. 7 B). Regarding blood lead levels, we observed that both lead exposures resulted in a significant increase in

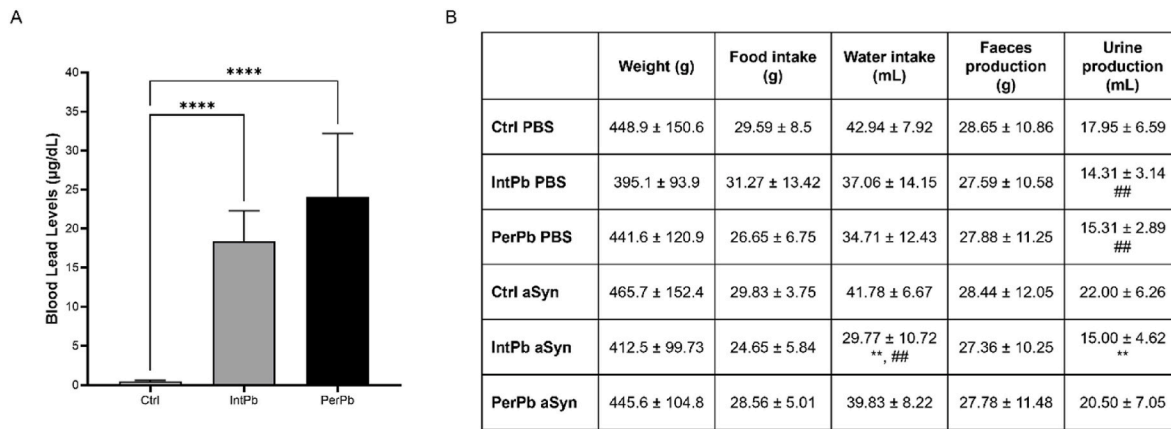


Fig. 7. Effect of lead exposure and aSyn PFF injection in the metabolic parameters. A. Histogram of the blood lead levels evaluated by atomic spectrophotometry; $F = 38.54$. B. Table with all data for the metabolic evaluation: weight, food and water intake, feces, and urine production. Values are the mean \pm SD ($n = 5-7$ for blood lead levels; $n = 16-20$ for metabolic data). The symbols denote statistically significant differences inter groups (Ctrl PBS vs IntPb PBS/PerPb PBS; Ctrl aSyn vs IntPb aSyn/PerPb aSyn - * $p < 0.05$, ** $p < 0.01$, *** $p < 0.001$, **** $p < 0.0001$; Ctrl PBS vs IntPb aSyn/PerPb aSyn; Ctrl aSyn vs IntPb PBS/PerPb PBS - # $p < 0.05$, ## $p < 0.01$, ### $p < 0.001$, #### $p < 0.0001$); two-way ANOVA, Tukey's multiple comparison test.

the BLL, with PerPb groups showing a higher level than IntPb (Fig. 7A).

3.7. Lead induces astrocytic atrophy alongside a reduction in aSyn pathology in the hippocampus

The morphological evaluation showed that lead-exposed groups without aSyn – IntPb PBS and PerPb PBS – showed a significant increase in the activation of the astrocytic cells, with hypertrophy of cellular processes and GFAP upregulation with a higher density of the astrocytic cells, confirming that astrocytes were in a reactive state (a hallmark of pathology). The same morphological changes were observed in the Ctrl aSyn group. IntPb aSyn and PerPb aSyn animals did not exhibit morphological alterations and were comparable to the Ctrl PBS group (Fig. 8A). Our quantitative analysis confirmed the morphological alterations observed. Specifically, we observed a significant increase in the percentage of GFAP-positive cells in both lead-exposed groups (without aSyn injection) when compared to the Ctrl PBS group. Interestingly, the lead exposed groups with aSyn showed a decrease when compared to Ctrl aSyn. Significant differences were also observed between IntPb PBS and IntPb aSyn, as well as in PerPb PBS and PerPb aSyn ($p < 0.0001$) with a significant decrease observed in the aSyn injected groups (Fig. 8B). We observed differences in fluorescence intensity and in GFP-positive cells (Fig. 8C–E). Altogether, these findings suggest aSyn may modify astrocytic responses, in a cross talk that has been reported by others (Forloni, 2023; Li et al., 2024).

3.8. Lead reduces dopaminergic neurons and aSyn levels in the substantia nigra and striatum

We observed a reduction in TH-positive cells in the intermittent lead exposure groups, and a slight increase in aSyn levels with the presence of lead or aSyn (Fig. 9A). The quantification of the images of the substantia nigra showed that the intermittent lead exposure, independent of the injection (PBS or aSyn) caused a significant decrease in the TH- positive cells when compared to the Ctrl PBS group (Fig. 9C). The quantification of the aSyn signal in the substantia nigra and striatum showed that, even though there is a minor increase in the fluorescence intensity, it is not significant in all groups, regardless of the lead exposure or the injection (Fig. 9D–E).

The morphological analysis of the paSyn-stained images showed that groups injected with aSyn display aSyn inclusion pathology in the substantia nigra region (yellow arrows that point to the inclusions), some of which occurs in dopaminergic (TH-positive) neurons (Fig. 9B). We observed no significant differences in paSyn S129 signal in substantia

nigra or striatum (Fig. 9F–G).

4. Discussion

We are living a PD “pandemic” that is proposed to be associated with the consequences of industrialization, i.e., environmental factors (Dorsey et al., 2018). In this context, heavy metals such as lead have been shown to act as toxicants in a variety of biological processes, increasing the risk for several age- and exposure-associated disorders. Several behavioral alterations associated with lead exposure in early life have been reported, including anxiety, locomotor dysfunction and memory impairment, manifesting years after the exposure (Chiodo et al., 2004; Honegger et al., 2011; Mason et al., 2014; Ortega et al., 2021; Sanders et al., 2009; Shvachiy et al., 2023; Toscano and Guilarte, 2005; Virgolini and Aschner, 2021). In the context of neurodegenerative diseases, most previous studies focused on AD, and on the effect of lead on A β and tau proteins, on epigenetics/DNA methylation, on protein expression and regulation, and on RNA biology (Bihaqi and Zawia, 2013; Eid et al., 2016; Masoud et al., 2018). Studies in humans suggested that exposure, even if only for short periods, increases the risk for PD (Coon et al., 2006; Gorell et al., 2006; Paul et al., 2021; Weisskopf et al., 2010b). However, the precise molecular mechanisms involved are unclear.

Here, we conducted a broad molecular and physiological assessment of the effect of lead exposure in cell and animal models of PD and related synucleinopathies. Importantly, we established new protocols to mimic different lead exposure profiles - permanent and intermittent low-level lead exposure - in cell cultures. We observed that both lead-exposure paradigms significantly increased aSyn inclusion formation. A similar effect was observed when adding lead to primary neuronal cultures for 16 days (from DIV5 to DIV21) treated with aSyn PFFs (Volpicelli-Daley et al., 2014). Nevertheless, we observed a stronger effect in the permanent lead exposure paradigm. Consistent with lead-associated neurotoxicity we observed signs of severe distress with axonal damage, consistent with effects on ion channels, signaling pathways, and mitochondrial function (Garza et al., 2006; Mason et al., 2014; Virgolini and Aschner, 2021; Zhang et al., 2011).

The precise effects of lead on aSyn-associated pathology are still elusive. However, lead causes an upregulation of aSyn and affects apoptosis mechanisms associated with tau pathology (Bihaqi et al., 2018). The formation of proteinaceous inclusions in response to lead exposure underscores the possible role of lead exposure in the origin and propagation of aSyn pathology (Goedert et al., 2017; Henderson et al., 2019; Iwatsubo, 2007; Murray et al., 2001). Consistently, our studies in animals revealed several changes in the presence of lead and/or aSyn

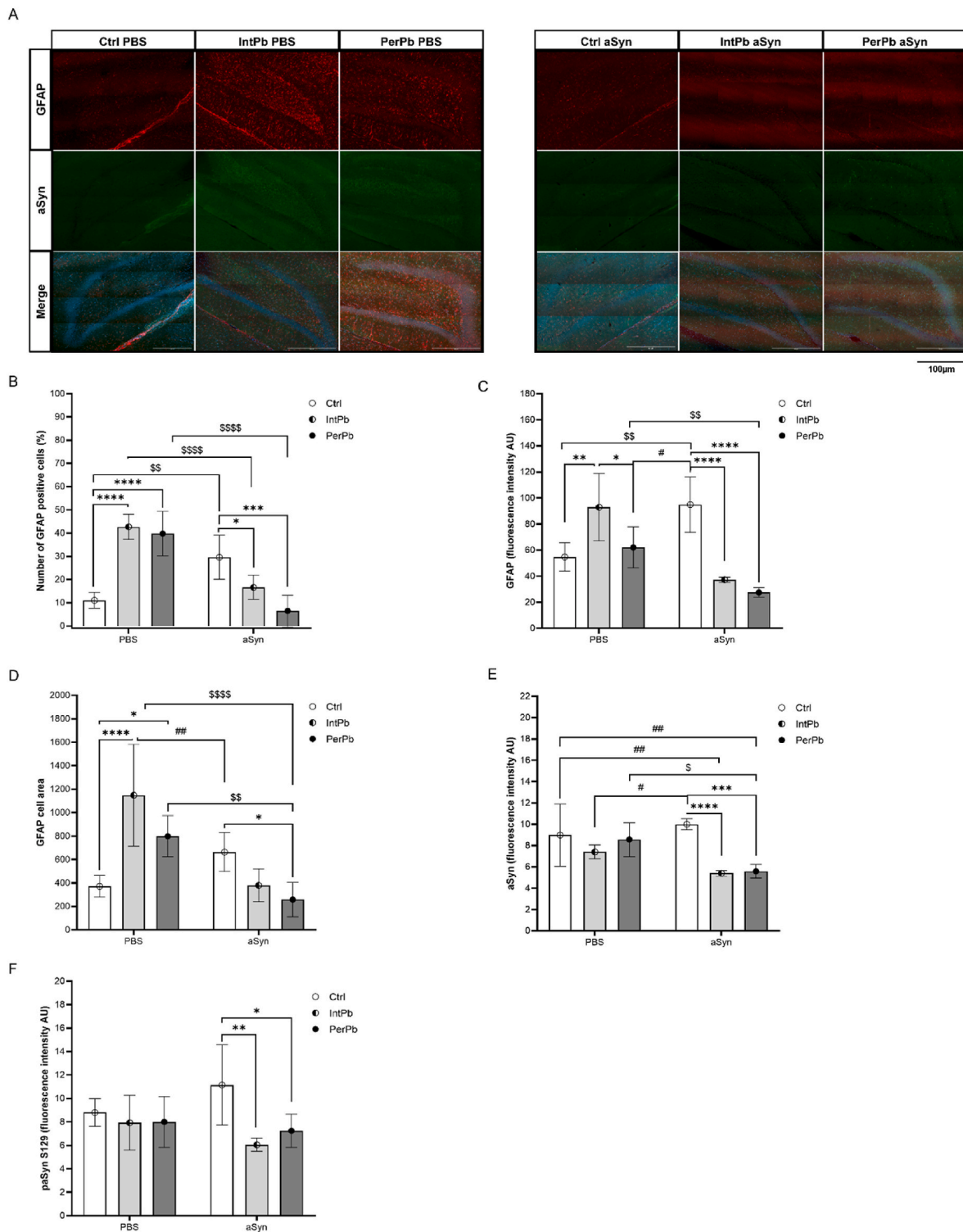


Fig. 8. Effect of lead and aSyn PFF injection on astrocytic activation, aSyn and paSyn S129 levels evaluated in dentate gyrus of the hippocampus. A. Representative images of the GFAP (1:1000)-stained astrocytes and aSynuclein (1:200). **B.** Histogram of the percentage of GFAP-positive cells' quantification; $F(2,32) = 38.92, p < 0.0001$. **C.** Histogram of GFAP fluorescence intensity quantification; $F(2,29) = 27.91, p < 0.0001$. **D.** Histogram of GFAP cell area quantification; $F(2,30) = 18.90, p < 0.0001$. **E.** Histogram of aSyn fluorescence intensity quantification; $F(2,30) = 6.353, p = 0.0050$. **F.** Histogram of paSyn S129 fluorescence intensity quantification; $F(2,30) = 3.374, p = 0.0477$. Images were acquired on a confocal point scanning microscope, (Zeiss LSM 900 with Airyscan 2), with a 20× objective for whole dentate gyrus imaging and a 63× objective for zooming in on the astrocytic cells. The scale bar is 100 μm or 50 μm for stained images. Values are the mean ± SD for n = 3–8 for all groups. The symbols denote statistically significant differences inter groups: Ctrl PBS vs IntPb PBS/PerPb PBS; Ctrl aSyn vs IntPb aSyn/PerPb aSyn - * $p < 0.05$, ** $p < 0.01$, *** $p < 0.001$, **** $p < 0.0001$; Ctrl PBS vs Ctrl aSyn/IntPb PBS vs IntPb aSyn/PerPb PBS - # $p < 0.05$, ## $p < 0.01$, ### $p < 0.001$, #### $p < 0.0001$; Ctrl PBS vs Ctrl aSyn/IntPb PBS vs IntPb aSyn/PerPb PBS vs PerPb aSyn - $^S p < 0.05$, $^{SS} p < 0.01$, $^{SSS} p < 0.001$, $^{SSSS} p < 0.0001$; two-way ANOVA, Tukey's multiple comparison test.

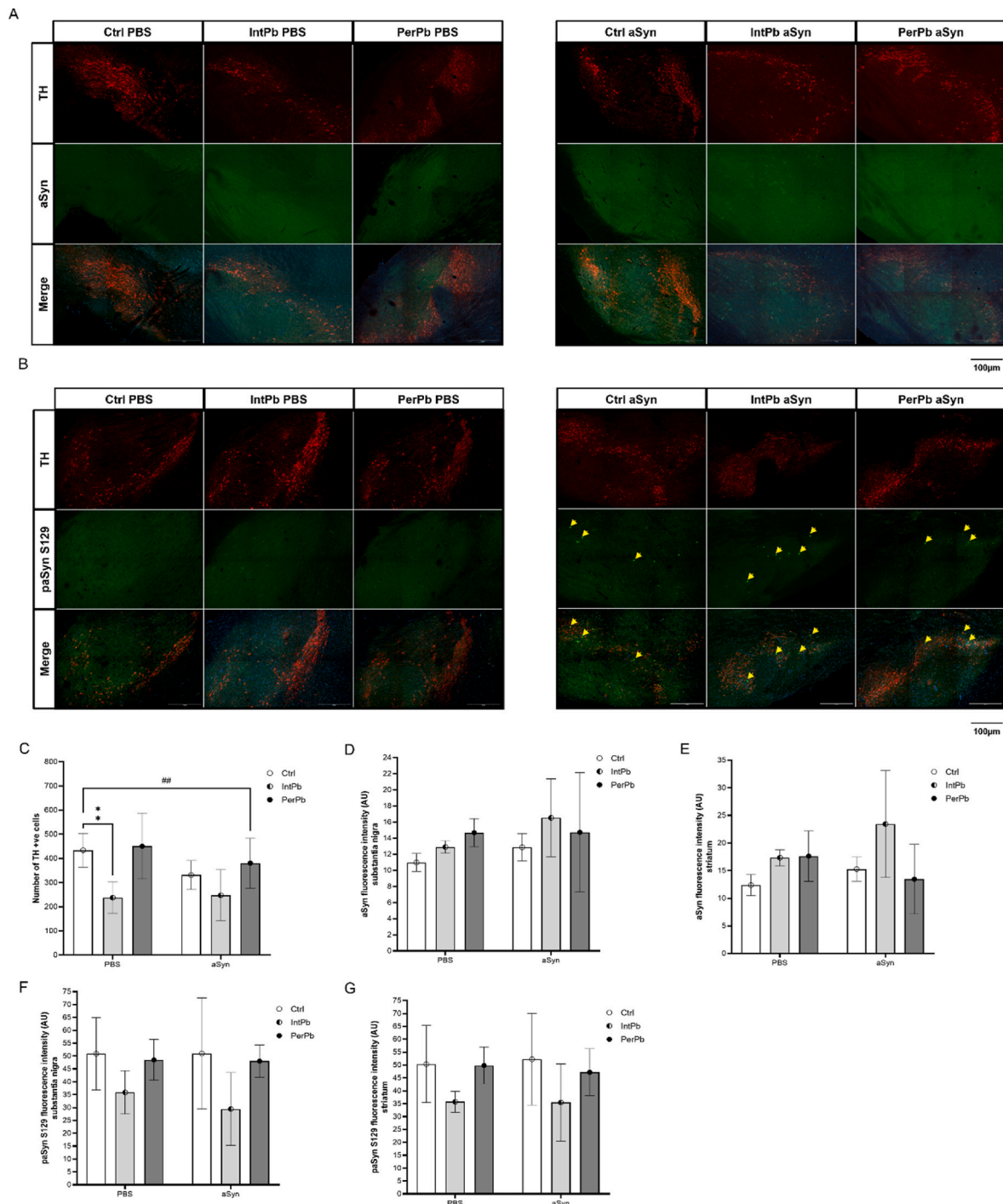


Fig. 9. Effect of lead and aSyn PFF injection on dopaminergic neurons (TH-positive cells), aSyn and paSyn S129 levels in the substantia nigra and striatum. A. Representative images of the TH (1:500)-stained dopaminergic neurons and aSyn (1:200) in the substantia nigra. B. Representative images of the TH (1:500)-stained dopaminergic neurons and paSyn S129 (1:200) in the substantia nigra. C. Histogram of the quantification of TH + ve cells; $F(2,42) = 1.335$, $p = 0.2742$. D. Histogram of quantification of aSyn fluorescence intensity in substantia nigra; $F(2,18) = 0.4495$, $p = 0.6449$. E. Histogram of quantification of aSyn fluorescence intensity in the striatum; $F(2,18) = 2.00$, $p = 0.1630$. F. Histogram of quantification of paSyn S129 fluorescence intensity in substantia nigra; $F(2,20) = 0.1659$, $p = 0.8483$. G. Histogram of quantification of paSyn S129 fluorescence intensity in striatum; $F(2,20) = 0.07963$, $p = 0.9238$. Images were acquired on a confocal point scanning microscope, (Zeiss LSM 900 with Airyscan 2), with a 10× objective. The scale bar is 100 μm for stained images. Values are the mean ± SD for $n = 4-8$ for all groups. The symbols denote statistically significant differences inter groups: Ctrl PBS vs IntPb PBS/PerPb PBS; Ctrl aSyn vs IntPb aSyn/PerPb aSyn - * $p < 0.05$, ** $p < 0.01$, *** $p < 0.001$, **** $p < 0.0001$; Ctrl PBS vs IntPb aSyn/PerPb aSyn; Ctrl aSyn vs IntPb PBS/PerPb PBS - # $p < 0.05$, ## $p < 0.01$, ### $p < 0.001$, #### $p < 0.0001$; two-way ANOVA, Tuckey's multiple comparison test.

injection in the striatum. We analyzed the behavior of at 28 weeks of age, after aSyn injection and with a long-term (28 weeks) lead exposure protocol to analyze the effects of the dual hit - lead and aSyn. We found that lead exposure has a strong effect on readouts of motor behavior, even in the absence of aSyn pathology. However, the strongest effect was observed in episodic long-term memory with a strong impairment observed in the intermittent and permanent lead-exposed groups. Although the effects of lead were observed even in the absence of aSyn pathology, environmental exposure to heavy metals and other toxicants can have an impact on aSyn, promoting more rapid progression of synucleinopathies and other neurodegenerative diseases (Cannon and Greenamyre, 2011; Chin-Chan et al., 2015; Mason et al., 2014; Nandipati and Litvan, 2016; Villar-Piqué et al., 2016).

Interestingly, we observed that all groups of animals treated with lead exhibited strong hypertension, with effects of both systolic and diastolic blood pressure and, consequently, in the mean blood pressure, without changes in the heart rate. Hypertension has been broadly associated with lead toxicity and in some forms of PD (Espay et al., 2016; Gonick et al., 1997; Grosu et al., 2023; Sharp et al., 1987; Vaziri, 2008; Yoo et al., 2021). Similarly, we also observed tachypnoea and chemoreceptor reflex hypersensitivity in the permanent lead exposure animals, regardless of aSyn injection, suggesting that the effects of lead on autonomic function may have occurred prior to aSyn injection. Likewise, and as previously described, we found that PerPb has a stronger effect on respiratory function and on autonomic control, indicating these animals are in a chronic alert-like state (Liana Shvachiy et al., 2020; Shvachiy et al., 2018, 2022). All cardiorespiratory changes observed are consistent with the blood levels of lead that were observed, with higher levels in the PerPb group which were above the levels considered safe by the World Health Organization (Organization, 2022; World Health Organization, 2010, 2021). Weight changes, which could be a confounding factor in behavioral and physiological alterations, were not present. However, we observed a slight decrease in water intake in the IntPb aSyn group together with a decrease in urine production in the group of animals treated with lead and aSyn, suggesting a slight change in the intake and excretion of lead (Han et al., 1999). These changes likely represent an adaptive response to lead intake or a consequence of lead-induced alterations in renal function and hydration regulation. While this study did not specifically quantify these effects, future investigations should consider metabolic and renal parameters to better understand the physiological impact of lead exposure on fluid balance (Toscano and Guilarte, 2005).

In terms of molecular alterations, we observed that lead caused a strong astrocytic activation in the hippocampus. The injection of aSyn did not exacerbate this effect. We found that some cells showed a “ghost-like” morphology, with atrophy of the cells and regression of the processes of the cells, an alteration that has been described before in PD and other diseases like Amyotrophic lateral sclerosis or frontotemporal dementia (Martin et al., 2001; Ramos-Gonzalez et al., 2021; Rossi et al., 2008; Wang et al., 2021). These cells have been hypothesized to take up lead prior to neurons, and to store it as a protective mechanism to neurons, similar to what happens with aSyn that is taken up by astrocytes from neuronal cells (Chen et al., 2015; Garza et al., 2006; Siracusa et al., 2019; Sofroniew and Vinters, 2010; Virgolini and Aschner, 2021; Wang et al., 2021).

Surprisingly, the levels of total aSyn and of paSyn (widely used as a marker of pathology) were slightly reduced in the hippocampus in animals treated with both lead and aSyn, independently of the type of lead exposure. This effect may be explained by the atrophy and reduced number of the astrocytic cells that we described previously in the hippocampus, compromising the retrieval of pathological forms of aSyn (He et al., 2021; Henderson et al., 2019; Pinho et al., 2019b). Similarly, we observed a strong degeneration of dopaminergic neurons (TH-positive cells) in the IntPb groups, and a slight decrease in these cells in the presence of aSyn alone in the *substantia nigra*, with a slight increase in the levels of aSyn in this brain region (Goedert et al., 2017; Henderson

et al., 2019; Murray et al., 2001; Radhakrishnan and Goyal, 2018; Spillantini and Goedert, 2000; Urbina et al., 2018).

In particular, the IntPb group injected with aSyn showed a decrease in paSyn levels, although we observed visible aSyn inclusions in dopaminergic neurons in the groups injected with aSyn. These observations confirm pathological alterations and suggest aSyn S129 phosphorylation may depend on the pathological insult (Majbour et al., 2016; Wang et al., 2021). In the striatum, where aSyn PFFs were injected, we observed an increase in the levels of aSyn in the groups injected; we found a trend showing higher levels of aSyn in the IntPb group, but this did not reach statistical significance and will have to be further evaluated in future studies. The distribution of the paSyn signal was similar to that in the *substantia nigra*, with a slight decrease in the IntPb group, possibly due to the loss of the dopaminergic neurons (Dehay and Bezard, 2019; Earls et al., 2019; Majbour et al., 2016; Paumier et al., 2015). It is possible that longer incubation times after aSyn PFF injection might lead to stronger effects, but this will have to be evaluated in future studies as it will involve a different protocol design.

While our study provides valuable insights into the potential effects of chronic Pb exposure on alpha-synuclein pathology, several limitations should be acknowledged. First, the use of human PFFs in a rodent model introduces potential differences in seeding efficiency and propagation rates, as homologous systems typically exhibit more efficient templating than heterologous ones. This may have influenced the extent of pathology observed. Additionally, while we assessed astrocytic and immune responses in selected brain regions, GFAP and microglial markers were not evaluated in the *striatum* or *substantia nigra*, limiting our ability to fully characterize neuroinflammatory changes in these areas. Future studies should include these markers to provide a more comprehensive understanding of Pb-induced effects on neuroinflammation. Furthermore, although chronic Pb exposure appeared to modulate astrocytic and immune responses, the lack of a clear additive effect on phosphorylated alpha-synuclein accumulation or behavioural outcomes suggests a complex interaction that requires further investigation. Lastly, total neuronal counts were not performed in the *substantia nigra*, making it unclear whether Pb exposure contributes to neurodegeneration or primarily affects tyrosine hydroxylase (TH) expression. Future studies employing stereological quantification and additional neuronal markers (e.g., NeuN) will help clarify this distinction. In summary, our results support a mechanistic correlation between environmental lead exposure and the onset and progression of diseases characterized by aSyn pathology accumulation, such as PD. Deciphering the intricate molecular and cellular interactions between lead and aSyn holds substantial implications for informing public health policies. Furthermore, such insights may offer novel perspectives on therapeutic strategies geared towards alleviating the effects of environmental toxicants on neurodegenerative processes, such as those manifesting in synucleinopathies.

CRediT authorship contribution statement

Liana Shvachiy: Writing – review & editing, Writing – original draft, Visualization, Validation, Methodology, Investigation, Formal analysis, Data curation, Conceptualization. **Ângela Amaro-Leal:** Writing – original draft, Visualization, Validation, Software, Methodology, Investigation, Formal analysis, Data curation, Conceptualization. **Filipa Machado:** Validation, Methodology, Investigation, Formal analysis, Data curation. **Isabel Rocha:** Writing – review & editing, Conceptualization. **Vera Geraldés:** Writing – review & editing, Validation, Supervision, Software, Resources, Project administration, Methodology, Funding acquisition, Conceptualization. **Tiago F. Outeiro:** Writing – review & editing, Validation, Supervision, Project administration, Funding acquisition, Conceptualization.

Institutional review board statement

The animal experimental protocol was in accordance with the

European and national law on animal welfare and was approved by the relevant local ethics committees. The primary cell cultures protocol was approved by the Lower Saxony State Office for Consumer Protection and Food Safety with the approval code 19/3213 and the animal behaviour and manipulation protocol had the approval of the ethics committee of the Academic Medical Center of Lisbon (CAML), Portugal with approval code 411/16.

Funding

L.S. was supported by the Foundation for Science and Technology (FCT), SFRH/BD/143286/2019. V.G. acknowledges the postdoctoral fellowship given by the Foundation for Science and Technology (FCT) (Ref: SFRH/BPD/119315/2016). T.F.O. is supported by the Deutsche Forschungsgemeinschaft (DFG, German Research Foundation) under Germany's Excellence Strategy, EXC 2067/1–390729940, and by SFB1286 (B8).

Declaration of competing interest

The authors declare the following financial interests/personal relationships which may be considered as potential competing interests: Liana Shvachiy reports financial support was provided by Foundation for Science and Technology. Tiago F. Outeiro reports financial support was provided by German Research Foundation. Vera Geraldine reports financial support was provided by Foundation for Science and Technology, Lisbon, Portugal. If there are other authors, they declare that they have no known competing financial interests or personal relationships that could have appeared to influence the work reported in this paper.

Acknowledgements

The authors would like to acknowledge the animal facility from the Faculty of Medicine of Lisbon, Portugal.

Data availability

The data presented in this study are available on request from the corresponding authors upon reasonable requests.

References

- Academy, A., Pediatrics, O.F., Exposure, L., 2005. Lead exposure in children: prevention, detection, and management. *Pediatrics* 116, 1036–1046. <https://doi.org/10.1542/peds.2005-1947>.
- Al-Azzani, M., König, A., Outeiro, T.F., 2022. Production of recombinant Alpha-Synuclein: still no standardized protocol in sight. *Biomolecules* 12. <https://doi.org/10.3390/biom12020324>.
- Antunes, M., Biala, G., 2012. The novel object recognition memory: neurobiology, test procedure, and its modifications. *Cogn. Process.* 13, 93–110. <https://doi.org/10.1007/s10339-011-0430-z>.
- Bihaqi, S.W., Zawia, N.H., 2013. Enhanced tauopathy and AD-like pathology in aged primate brains decades after infantile exposure to lead (Pb). *Neurotoxicology* 39, 95–101. <https://doi.org/10.1016/j.neuro.2013.07.010>.
- Bihaqi, S.W., Alansi, B., Masoud, A.M., Mushtaq, F., Subaiea, G.M., Zawia, N.H., 2018. Influence of early life lead (Pb) exposure on α -Synuclein, GSK-3 β and Caspase-3 mediated tauopathy: implications on alzheimer's disease. *Curr. Alzheimer Res.* 15, 1114–1122. <https://doi.org/10.2174/1567205015666180801095925>.
- Braak, H., Del, K., Rüb, U., Vos, R.A.I. de, Jansen, E.N.H., Braak, E., 2003. Braak H, 2003. pdf, pp. 197–211. [https://doi.org/10.1016/S0197-4580\(02\)00065-9](https://doi.org/10.1016/S0197-4580(02)00065-9).
- Buccafusco, Jerry J., 2001. Methods of Behavior Analysis in Neurosciences. CRC Press LLC, New York. [https://doi.org/10.1016/0005-7916\(93\)90032-R](https://doi.org/10.1016/0005-7916(93)90032-R).
- Caldeira Brás, I., Hossein Khani, M., Vasilis, E., Möbius, W., Riedel, D., Parfentev, I., Gerhardt, E., Fahlbusch, C., Urlaub, H., Zweckstetter, M., Gollisch, T., Fleming Outeiro, T., n.d. Common molecular mechanisms underlie the transfer of alpha-synuclein, Tau and huntingtin and modulate spontaneous activity in neuronal cells. <https://doi.org/10.1101/2021.07.18.452825>.
- Cannon, J.R., Greenamyre, J.T., 2011. The role of environmental exposures in neurodegeneration and neurodegenerative diseases. *Toxicol. Sci.* 124, 225–250. <https://doi.org/10.1093/toxsci/kfr239>.
- Chegão, A., Guarda, M., Alexandre, B.M., Shvachiy, L., Temido-Ferreira, M., Marques-Morgado, I., Fernandes Gomes, B., Matthiesen, R., Lopes, L. V., Florindo, P.R., Anjos

- Gomes, R., Gomes-Alves, P., Coelho, J.E., Outeiro, F., Miranda, H.V., n.d. Glycation modulates glutamatergic signalling and exacerbates Parkinson's disease-like phenotypes. <https://doi.org/10.1101/2021.08.24.457507>.
- Chen, L.-W., Dong, M.-H., Kuang, F., Liu, J.-T., Zhang, J.-Q., Bai, Y., 2015. Microglia and astroglia: the role of neuroinflammation in lead toxicity and neuronal injury in the brain. *Neuroimmunol. Neuroinflammation* 2, 131. <https://doi.org/10.4103/2347-8659.156980>.
- Chen, Z., Li, G., Liu, J., 2020. Autonomic dysfunction in Parkinson's disease: implications for pathophysiology, diagnosis, and treatment. *Neurobiol. Dis.* <https://doi.org/10.1016/j.nbd.2019.104700>.
- Chin-Chan, M., Navarro-Yepes, J., Quintanilla-Vega, B., 2015. Environmental pollutants as risk factors for neurodegenerative disorders: alzheimer and Parkinson diseases. *Front. Cell. Neurosci.* 9, 124. <https://doi.org/10.3389/FNCEL.2015.00124/BIBTEX>.
- Chiodo, L.M., Jacobson, S.W., Jacobson, J.L., 2004. Neurodevelopmental effects of postnatal lead exposure at very low levels. *Neurotoxicol. Teratol.* 26, 359–371. <https://doi.org/10.1016/j.ntt.2004.01.010>.
- Coon, E.A., Singer, W., 2020. Synucleinopathies. *CONTINUUM* lifelong learning in neurology. <https://doi.org/10.1212/CON.0000000000000819>.
- Coon, S., Stark, A., Peterson, E., Gloi, A., Kortsha, G., Pounds, J., Chettle, D., Gorell, J., 2006. Whole-body lifetime occupational lead exposure and risk of Parkinson's disease. *Environ. Health Perspect.* 114, 1872–1876. <https://doi.org/10.1289/EHP.9102>.
- Costa, R., Tamascia, M.L., Nogueira, M.D., Casarini, D.E., Marcondes, F.K., 2012. Handling of adolescent rats improves learning and memory and decreases anxiety. *JAALAS* 51, 548–553.
- Creed, R.B., Goldberg, M.S., 2018. New developments in genetic rat models of Parkinson's disease. *Mov. Disord.* <https://doi.org/10.1002/mds.27296>.
- Deacon, R.M.J., 2013. Measuring motor coordination in mice. *J. Vis. Exp.* <https://doi.org/10.3791/2609>.
- Dehay, B., Bezard, E., 2019. Intrastriatal injection of alpha-synuclein fibrils induces Parkinson-like pathology in macaques. *Brain.* <https://doi.org/10.1093/brain/awz329>.
- Dorsey, E.R., Sherer, T., Okun, M.S., Bloem, B.R., 2018. The emerging evidence of the parkinson pandemic. *J. Parkinsons Dis.* 8, S3–S8. <https://doi.org/10.3233/JPD-181474>.
- Earls, R.H., Menees, K.B., Chung, J., Barber, J., Gutekunst, C.A., Hazim, M.G., Lee, J.K., 2019. Intrastriatal injection of preformed alpha-synuclein fibrils alters central and peripheral immune cell profiles in non-transgenic mice. *J. Neuroinflammation* 16. <https://doi.org/10.1186/s12974-019-1636-8>.
- Eid, A., Bihaqi, S.W., Renehan, W.E., Zawia, N.H., 2016. Developmental lead exposure and lifespan alterations in epigenetic regulators and their correspondence to biomarkers of Alzheimer's disease. *Alzheimer's and Dementia: Diagnosis, Assessment and Disease Monitoring* 2, 123–131. <https://doi.org/10.1016/j.dadm.2016.02.002>.
- Elfil, M., Kamel, S., Kandil, M., Koo, B.B., Schaefer, S.M., 2020. Implications of the gut microbiome in parkinson's disease. *Mov. Disord.* <https://doi.org/10.1002/mds.28004>.
- Espay, A.J., LeWitt, P.A., Hauser, R.A., Merola, A., Masellis, M., Lang, A.E., 2016. Neurogenic orthostatic hypotension and supine hypertension in Parkinson's disease and related synucleinopathies: prioritisation of treatment targets. *Lancet Neurol.* [https://doi.org/10.1016/S1474-4422\(16\)30079-5](https://doi.org/10.1016/S1474-4422(16)30079-5).
- Fleming, S.M., 2011. Cardiovascular autonomic dysfunction in animal models of parkinson's disease. *J. Parkinsons Dis.* <https://doi.org/10.3233/JPD-2011-11042>.
- Flora, G., Gupta, D., Tiwari, A., 2012. Toxicity of lead: a review with recent updates. *Interdiscip. Toxicol.* 5, 47–58. <https://doi.org/10.2478/v10102-012-0009-2>.
- Forloni, G., 2023. Alpha synuclein: neurodegeneration and inflammation. *Int. J. Mol. Sci.* <https://doi.org/10.3390/ijms24065914>.
- Garza, A., Vega, R., Soto, E., 2006. Cellular mechanisms of lead neurotoxicity. *Med. Sci. Monit.* 12, 57–65.
- Geraldes, V., Carvalho, M., Goncalves-Rosa, N., Tavares, C., Laranjo, S., Rocha, I., 2016. Lead toxicity promotes autonomic dysfunction with increased chemoreceptor sensitivity. *Neurotoxicology* 54, 170–177. <https://doi.org/10.1016/j.neuro.2016.04.016>.
- Gidlow, D.A., 2015. Lead toxicity. *Occup. Med.* 65, 348–356.
- Goedert, M., Jakes, R., Spillantini, M.G., 2017. The synucleinopathies: twenty years on. *J. Parkinsons Dis.* <https://doi.org/10.3233/JPD-179005>.
- Goldstein, D.S., 2013. Cardiovascular autonomic dysfunction in Parkinson's disease. *Parkinson's Disease and Nonmotor Dysfunction (Second Edition 289)*, 201–212. https://doi.org/10.1007/978-1-60761-429-6_13.
- Gonick, H.C., Ding, Y., Bondy, S.C., Ni, Z., Vaziri, N.D., 1997. Lead-induced hypertension. *Hypertension* 30, 1487–1492.
- Gorell, J.M., Johnson, C.C., Rybicki, B.A., Peterson, E.L., Kortsha, G.X., Brown, G.G., Richardson, R.J., Gorell, Jay M., 1997. Occupational Exposures to Metals as Risk Factors for Parkinson's Disease.
- Gorell, J., Kortsha, G., Stark, A., Peterson, E., Pounds, J., Chettle, D., Gloi, A., Coon, S., 2006. Whole-body lifetime occupational lead exposure and risk of parkinson's disease. *Environ. Health Perspect.* 114, 1872–1876. <https://doi.org/10.1289/ehp.9102>.
- Grosu, L., Grosu, A.I., Crisan, D., Zlibut, A., Perju-Dumbrava, L., 2023. Parkinson's disease and cardiovascular involvement: edifying insights. *Biomed Rep* 18. <https://doi.org/10.3892/br.2023.1607> submitted for publication.
- Guimarães, D., Carvalho, M.L., Geraldes, V., Rocha, I., Alves, L.C., Santos, J.P., 2012. Lead in liver and kidney of exposed rats: aging accumulation study. *J. Trace Elem. Med. Biol.* 26, 285–290. <https://doi.org/10.1016/j.jtemb.2012.02.006>.
- Han, S., Li, W., Jamil, U., Dargan, K., Orefice, M., Kemp, F.W., Bogden, J.D., 1999. Effects of weight loss and exercise on the distribution of lead and essential trace elements in

- rats with prior lead exposure. *Environ. Health Perspect.* 107, 657–662. <https://doi.org/10.1289/ehp.99107657>.
- Hawkes, C.H., del Tredici, K., Braak, H., 2010. A timeline for Parkinson's disease. *Park. Relat. Disord.* 16, 79–84. <https://doi.org/10.1016/j.parkrel.2009.08.007>.
- He, S., Zhong, S., Liu, G., Yang, J., 2021. Alpha-synuclein: the interplay of pathology, neuroinflammation, and environmental factors in parkinson's disease. *Neurodegener. Dis.* <https://doi.org/10.1159/000511083>.
- Henderson, M.X., Trojanowski, J.Q., Lee, V.M.Y., 2019. α -Synuclein pathology in Parkinson's disease and related α -synucleinopathies. *Neurosci. Lett.* 709, 134316. <https://doi.org/10.1016/j.neulet.2019.134316>.
- Hol, E.M., Pekny, M., 2015. Glial fibrillary acidic protein (GFAP) and the astrocyte intermediate filament system in diseases of the central nervous system. *Curr. Opin. Cell Biol.* 32, 121–130. <https://doi.org/10.1016/j.cceb.2015.02.004>.
- Honegger, P., Corbaz, A., Zurich, M.-G., Monnet-Tschudi, F., Boschat, C., 2011. Involvement of environmental mercury and lead in the etiology of neurodegenerative diseases. *Rev. Environ. Health* 21. <https://doi.org/10.1515/reveh.2006.21.2.105>.
- Iwatsubo, T., 2007. Pathological biochemistry of α -synucleinopathy. *Neuropathology* 474–478. <https://doi.org/10.1111/j.1440-1789.2007.00785.x>.
- Koller, K., Brown, T., Spurgeon, A., Levy, L., 2004. Recent developments in low-level lead exposure and intellectual impairment in children. *Environ. Health Perspect.* 112, 987–994. <https://doi.org/10.1289/ehp.6941>.
- Laura Mayans, n.d. Lead Poisoning in Children.
- Laurent, C., Burnouf, S., Ferry, B., Batalha, V.L., Coelho, J.E., Baqi, Y., Malik, E., Marciniaik, E., Parrot, S., Van Der Jeugd, A., Faivre, E., Flaten, V., Ledent, C., D'Hooge, R., Sergeant, N., Hamdane, M., Humez, S., Müller, C.E., Lopes, L.V., Buée, L., Blum, D., 2016. A2A adenosine receptor deletion is protective in a mouse model of tauopathy. *Mol. Psychiatry* 21, 97–107. <https://doi.org/10.1038/mp.2014.151>.
- Lázaro, D.F., Pavlou, M.A.S., Outeiro, T.F., 2017. Cellular models as tools for the study of the role of alpha-synuclein in Parkinson's disease. *Exp. Neurol.* 298, 162–171. <https://doi.org/10.1016/j.jepneuro.2017.05.007>.
- Li, K., Ling, H., Huang, W., Luo, W., Gu, C., Tao, B., Xie, Q., Qiu, P., 2024. Single-cell RNA-sequencing analysis reveals α -syn induced astrocyte-neuron crosstalk-mediated neurotoxicity. *Int. Immunopharmacol.* 139, 112676. <https://doi.org/10.1016/j.intimp.2024.112676>.
- Lubrich, C., Giesler, P., Kipp, M., 2022. Motor behavioral deficits in the cuprizone model: validity of the rotarod test paradigm. *Int. J. Mol. Sci.* <https://doi.org/10.3390/ijms231911342>.
- Majbour, N.K., Vaikath, N.N., Van Dijk, K.D., Ardah, M.T., Varghese, S., Vesterager, L.B., Montezinho, L.P., Poole, S., Safieh-Garabedian, B., Tokuda, T., Teunissen, C.E., Berendse, H.W., Van De Berg, W.D.J., El-Agnaf, O.M.A., 2016. Oligomeric and phosphorylated alpha-synuclein as potential CSF biomarkers for Parkinson's disease. *Mol. Neurodegener.* 11. <https://doi.org/10.1186/s13024-016-0072-9>.
- Marques, O., Outeiro, T.F., 2012. Alpha-synuclein: from secretion to dysfunction and death. *Cell Death Dis.* 3. <https://doi.org/10.1038/cddis.2012.94>.
- Martin, J.A., Craft, D.K., Su, J.H., Kim, R.C., Cotman, C.W., 2001. Astrocytes degenerate in frontotemporal dementia: possible relation to hypoperfusion. *Neurobiol. Aging* 22, 195–207.
- Mason, L.H., Harp, J.P., Han, D.Y., Mason, L.H., Harp, J.P., Han, D.Y., 2014. Pb neurotoxicity: neuropsychological effects of lead toxicity. *BioMed Res. Int.* 2014, 1–8. <https://doi.org/10.1155/2014/840547>.
- Masoud, A.M., Bihagi, S.W., Alansi, B., Dash, M., Subaiea, G.M., Renhan, W.E., Zawia, N.H., 2018. Altered microRNA, mRNA, and protein expression of neurodegeneration-related biomarkers and their transcriptional and epigenetic modifiers in a human tau transgenic mouse model in response to developmental lead exposure. *J. Alzheimers Dis* 63, 273–282. <https://doi.org/10.3233/JAD-170824>.
- McLean, P.J., Kawamata, H., Hyman, B.T., 2001. α -Synuclein-enhanced green fluorescent protein fusion proteins form proteasome sensitive inclusions in primary neurons. *Neuroscience* 104, 901–912. [https://doi.org/10.1016/S0306-4522\(01\)00113-0](https://doi.org/10.1016/S0306-4522(01)00113-0).
- Mehra, S., Sahay, S., Maji, S.K., 2019. α -Synuclein misfolding and aggregation: implications in Parkinson's disease pathogenesis. *Biochim. Biophys. Acta Proteins Proteom.* <https://doi.org/10.1016/j.bbapap.2019.03.001>.
- Moreira, E.G., Vassilief, I., Vassilief, V.S., 2001. Developmental lead exposure: behavioral alterations in the short and long term. *Neurotoxicol. Teratol.* 23, 489–495. [https://doi.org/10.1016/S0892-0362\(01\)00159-3](https://doi.org/10.1016/S0892-0362(01)00159-3).
- Mouro, F.M., Batalha, V.L., Ferreira, D.G., Coelho, J.E., Baqi, Y., Müller, C.E., Lopes, L.V., Ribeiro, J.A., Sebastião, A.M., 2017. Chronic and acute adenosine A2A receptor blockade prevents long-term episodic memory disruption caused by acute cannabinoid CB1 receptor activation. *Neuropharmacology* 117, 316–327. <https://doi.org/10.1016/j.neuropharm.2017.02.021>.
- Murray, I.V., M-Y Lee, V., Trojanowski, J.Q., 2001. Synucleinopathies: a pathological and molecular review. *Clin. Neurosci. Res.* 445–455.
- Nandipati, S., Litvan, I., 2016. Environmental exposures and parkinson's disease. *Int. J. Environ. Res. Publ. Health* 13. <https://doi.org/10.3390/IJERPH13090881>.
- Naolapo, O.J.O., Naolapo, A.Y.O., Josiah, T., Osaku, M., Akanji, O.O., Abiodun, O.R., 2012. Elevated plus maze and Y-Maze behavioral effects of subchronic, oral low dose monosodium glutamate in Swiss albino mice. *Journal of Pharmacy and Biological Sciences* 3, 21–27. <https://doi.org/10.9790/3008-0342127>.
- Ogun, S.A., 2002. Parkinson's disease - a review. *Afr. J. Neurol. Sci.* 21, 65–74.
- Organization, W.H., 2022. Lead poisoning and health [WWW Document]. Fact sheet. URL <https://www.who.int/news-room/fact-sheets/detail/lead-poisoning-and-health>. (Accessed 8 July 2023).
- Ortega, D.R., Esquivel, D.F.G., Ayala, T.B., Pineda, B., Manzo, S.G., Quino, J.M., Mora, P. C., Cruz, V.P. de la, 2021. Cognitive impairment induced by lead exposure during lifespan: mechanisms of lead neurotoxicity, 2021 *Toxics* 9, 23. <https://doi.org/10.3390/TOXICS9020023>, 9, 23.
- Parsian, H., Alipour, P., Gholinia, H., Saadat, P., 2021. Comparison of serum lead and cadmium levels in parkinson's patients and healthy controls. *Arch. Neurosci* 8. <https://doi.org/10.5812/ans.103376>.
- Paul, K.C., Horvath, S., Del Rosario, I., Bronstein, J.M., Ritz, B., 2021. DNA methylation biomarker for cumulative lead exposure is associated with Parkinson's disease. *Clin. Epigenet.* 13. <https://doi.org/10.1186/S13148-021-01051-3>.
- Paumier, K.L., Luk, K.C., Manfredsson, F.P., Kanaan, N.M., Lipton, J.W., Collier, T.J., Steece-Collier, K., Kemp, C.J., Celano, S., Schulz, E., Sandoval, I.M., Fleming, S., Dirr, E., Polinski, N.K., Trojanowski, J.Q., Lee, V.M., Sortwell, C.E., 2015. Intra-atrial injection of pre-formed mouse α -synuclein fibrils into rats triggers α -synuclein pathology and bilateral nigrostriatal degeneration. *Neurobiol. Dis.* 82, 185–199. <https://doi.org/10.1016/j.NBD.2015.06.003>.
- Pinho, R., Paiva, I., Jerčić, K.G., Fonseca-Ornelas, L., Gerhardt, E., Fahlbusch, C., Garcia-Esparcia, P., Kerimoglu, C., Pavlou, M.A.S., Villar-Piqué, A., Szegő, É., Lopes Da Fonseca, T., Odoardi, F., Soeroes, S., Rego, A.C., Fischle, W., Schwamborn, J.C., Meyer, T., Kügler, S., Ferrer, I., Attems, J., Fischer, A., Becker, S., Zweckstetter, M., Borovecki, F., Outeiro, T.F., 2019a. Nuclear localization and phosphorylation modulate pathological effects of alpha-synuclein. *Hum. Mol. Genet.* 28, 31–50. <https://doi.org/10.1093/hmg/ddy326>.
- Pinho, R., Paiva, I., Jerčić, K.G., Fonseca-Ornelas, L., Gerhardt, E., Fahlbusch, C., Garcia-Esparcia, P., Kerimoglu, C., Pavlou, M.A.S., Villar-Piqué, A., Szegő, É., Lopes Da Fonseca, T., Odoardi, F., Soeroes, S., Rego, A.C., Fischle, W., Schwamborn, J.C., Meyer, T., Kügler, S., Ferrer, I., Attems, J., Fischer, A., Becker, S., Zweckstetter, M., Borovecki, F., Outeiro, T.F., 2019b. Nuclear localization and phosphorylation modulate pathological effects of alpha-synuclein. *Hum. Mol. Genet.* 28, 31–50. <https://doi.org/10.1093/hmg/ddy326>.
- Radhakrishnan, D., Goyal, V., 2018. Parkinson's disease: a review. *Neurol. India* 66, 26. <https://doi.org/10.4103/0028-3886.226451>.
- Ramos, A., 2008. Animal models of anxiety: do I need multiple tests? *Trends Pharmacol. Sci.* 29, 493–498. <https://doi.org/10.1016/j.tips.2008.07.005>.
- Ramos-Gonzalez, P., Mato, S., Chara, J.C., Verkhratsky, A., Matute, C., Cavaliere, F., 2021. Astrocytic atrophy as a pathological feature of Parkinson's disease with LRRK2 mutation. *npj Parkinson's Dis.* 7. <https://doi.org/10.1038/s41531-021-00175-w>.
- Rocha, A., Trujillo, K.A., 2019. Neurotoxicity of low-level lead exposure: history, mechanisms of action, and behavioral effects in humans and preclinical models. *Neurotoxicology.* <https://doi.org/10.1016/j.neuro.2019.02.021>.
- Rossi, D., Brambilla, L., Valori, C.F., Roncoroni, C., Crugnola, A., Yokota, T., Bredesen, D. E., Volterra, A., 2008. Focal degeneration of astrocytes in amyotrophic lateral sclerosis. *Cell Death Differ.* 15, 1691–1700. <https://doi.org/10.1038/cdd.2008.99>.
- Sanders, T., Liu, Y., Buchner, V., Tchounvout, P.B., 2009. Neurotoxic effects and biomarkers of lead exposure: a review. *Rev. Environ. Health* 24, 15–46.
- Sani, A.H., Amanabo, M., 2021. Lead: a concise review of its toxicity, mechanism and health effect. <https://doi.org/10.30574/gscbps.2021.15.1.0096>.
- Santos Alves, Rogério dos, de Souza, Alex Soares, et al., 2014. The open field test. *Igars* 1–5. <https://doi.org/10.1007/s13398-014-0173-7>, 2014.
- Schindelin, J., Arganda-Carreras, I., Frise, E., Kaynig, V., Longair, M., Pietzsch, T., Preibisch, S., Rueden, C., Saalfeld, S., Schmid, B., Tinevez, J.-Y., White, D.J., Hartenstein, V., Eliceiri, K., Tomancak, P., Cardona, A., 2012. Fiji: an open-source platform for scientific image analysis. *Nat. Methods* 9, 676–682.
- Schmitt, U., Hiemke, C., 1998. Strain differences in open-field and elevated plus-maze behavior of rats without and with pretest handling. *Pharmacol. Biochem. Behav.* 59, 807–811. [https://doi.org/10.1016/S0091-3057\(97\)00502-9](https://doi.org/10.1016/S0091-3057(97)00502-9).
- Scorza, F.A., Fiorini, A.C., Scorza, C.A., Finsterer, J., 2018. Cardiac abnormalities in Parkinson's disease and parkinsonism. *J. Clin. Neurosci.* <https://doi.org/10.1016/j.jocn.2018.04.031>.
- Sharp, D.S., Becker, C.E., Smith, A.H., 1987. Chronic low-level lead exposure: its role in the pathogenesis of hypertension. *Med Toxicol Adverse Drug Exp* 2, 210–232. <https://doi.org/10.1007/BF03259865>.
- Shvachiy, L., Gerales, V., Amaro-Leal, Á., Rocha, I., 2018. Intermittent low-level lead exposure provokes anxiety, hypertension, autonomic dysfunction and neuroinflammation. *Neurotoxicology* 69, 307–319. <https://doi.org/10.1016/j.neuro.2018.08.001>.
- Shvachiy, Liana, Gerales, V., Amaro-Leal, Á., Rocha, I., 2020. Persistent effects on cardiorespiratory and nervous systems induced by long-term lead exposure: results from a longitudinal study. *Neurotox. Res.* 37, 857–870. <https://doi.org/10.1007/s12640-020-00162-8>.
- Shvachiy, L., Amaro-Leal, Á., Outeiro, T.F., Rocha, I., Gerales, V., 2022. From molecular to functional effects of different environmental lead exposure paradigms. *Biology* 11, 1164. <https://doi.org/10.3390/BIOLOGY11081164>, 11, 1164.
- Shvachiy, L., Amaro-Leal, Á., Outeiro, T.F., Rocha, I., Gerales, V., 2023. Intermittent lead exposure induces behavioral and cardiovascular alterations associated with neuroinflammation. *Cells* 12. <https://doi.org/10.3390/cells12050818>.
- Siracusa, R., Fusco, R., Cuzzocrea, S., 2019. Astrocytes: role and functions in brain pathologies. *Front. Pharmacol.* 10. <https://doi.org/10.3389/fphar.2019.01114>.
- Sofroniew, M.V., Vinters, H.V., 2010. Astrocytes: biology and pathology. *Acta Neuropathol.* 119, 7–35. <https://doi.org/10.1007/s00401-009-0619-8>.
- Spillantini, M.G., Goedert, M., 2000. The α -Synucleinopathies: parkinson's disease, dementia with lewy bodies, and multiple system atrophy. *Ann. N. Y. Acad. Sci.* 920, 16–27. <https://doi.org/10.1111/J.1749-6632.2000.TB06900.X>.
- Tempowski, J., 2021. WHO Guideline for Clinical Management of Exposure to Lead. World Health Organization.
- Todd, A.C., Wetmur, J.G., Moline, J.M., Godbold, J.H., Levin, S.M., Landrigan, P.J., 1996. Unraveling the chronic toxicity of lead: an essential priority for environmental

- health. *Environ. Health Perspect.* 104, 141–146. <https://doi.org/10.1289/ehp.96104s1141>.
- Toscano, C.D., Guillarte, T.R., 2005. Lead neurotoxicity: from exposure to molecular effects. *Brain Res. Rev.* 49, 529–554. <https://doi.org/10.1016/j.brainresrev.2005.02.004>.
- Urbina, M.A., Chirumbolo, S., Stejskal, V., Bjorklund, G., Mutter, J., Dadar, M., 2018. Metals and parkinson's disease: mechanisms and biochemical processes. *Curr. Med. Chem.* 25, 2198–2214. <https://doi.org/10.2174/0929867325666171129124616>.
- Vaziri, N.D., 2008. Mechanisms of lead-induced hypertension and cardiovascular disease. *Am. J. Physiol. Heart Circ. Physiol.* 295, H454–H465. <https://doi.org/10.1152/ajpheart.00158.2008>.
- Villar-Piqué, A., Da Fonseca, T.L., Sant'Anna, R., Szegő, É.M., Fonseca-Ornelas, L., Pinho, R., Carija, A., Gerhardt, E., Masaracchia, C., Gonzalez, E.A., Rossetti, G., Carloni, P., Fernández, C.O., Foguel, D., Milosevic, I., Zweckstetter, M., Ventura, S., Outeiro, T.F., 2016. Environmental and genetic factors support the dissociation between α -synuclein aggregation and toxicity. *Proc. Natl. Acad. Sci. U. S. A.* 113, E6506–E6515. <https://doi.org/10.1073/pnas.1606791113>.
- Virgolini, M.B., Aschner, M., 2021. Molecular mechanisms of lead neurotoxicity. In: *Advances in Neurotoxicology*. Elsevier Inc., pp. 159–213. <https://doi.org/10.1016/bs.ant.2020.11.002>
- Volpicelli-Daley, L.A., Luk, K.C., Lee, V.M.-Y., 2014. Addition of exogenous α -synuclein preformed fibrils to primary neuronal cultures to seed recruitment of endogenous α -synuclein to lewy body and lewy neurite-like aggregates. *Nat. Protoc.* 9, 2135–2146. <https://doi.org/10.1038/nprot.2014.143>.
- Wang, C., Yang, T., Liang, M., Xie, J., Song, N., 2021. Astrocyte dysfunction in Parkinson's disease: from the perspectives of transmitted α -synuclein and genetic modulation. *Transl. Neurodegener.* <https://doi.org/10.1186/s40035-021-00265-y>.
- Wani, A.L., Ara, A., Usmani, J.A., 2015. Lead toxicity: a review. *Interdiscip Toxicol.* <https://doi.org/10.1515/intox-2015-0009>.
- Waseem, S., Bahmani, A., Subaiea, G.M., Zawia, N.H., 2014. Infantile exposure to lead and late-age cognitive decline : relevance to AD. *Alzheimer's Dementia* 10, 187–195. <https://doi.org/10.1016/j.jalz.2013.02.012>.
- Weisskopf, M.G., Weuve, J., Nie, H., Saint-Hilaire, M.H., Sudarsky, L., Simon, D.K., Hersh, B., Schwartz, J., Wright, R.O., Hu, H., 2010a. Association of cumulative lead exposure with Parkinson's disease. *Environ. Health Perspect.* 118, 1609–1613. <https://doi.org/10.1289/ehp.1002339>.
- Weisskopf, M.G., Weuve, J., Nie, H., Saint-Hilaire, M.-H., Sudarsky, L., Simon, D.K., Hersh, B., Schwartz, J., Wright, R.O., Hu, H., 2010b. Association of cumulative lead exposure with parkinson's disease. *Environ. Health Perspect.* 118, 1609–1613. <https://doi.org/10.1289/EHP.1002339>.
- Wong, Y.C., Krainc, D., 2017. α -synuclein toxicity in neurodegeneration: mechanism and therapeutic strategies. *Nat. Med.* 23, 1–13. <https://doi.org/10.1038/nm.4269>.
- World Health Organization, 2010. Exposure to lead: a major public health concern. World Health Organization 6. <https://doi.org/10.1016/j.ecoenv.2011.12.007>.
- World Health Organization, 2021. Exposure to lead: a major public health concern. In: *Preventing Disease Through Healthy Environments, second ed.* Geneva.
- Wu, J., Basha, M.R., Brock, B., Cox, D.P., Cardozo-Pelaez, F., McPherson, C.A., Harry, J., Rice, D.C., Maloney, B., Chen, D., Lahiri, D.K., Zawia, N.H., 2008. Alzheimer's disease (AD)-like pathology in aged monkeys after infantile exposure to environmental metal lead (Pb): evidence for a developmental origin and environmental link for AD. *J. Neurosci.* 28, 3–9. <https://doi.org/10.1523/JNEUROSCI.4405-07.2008>.
- Yoo, S.W., Kim, J.S., Oh, Y.S., Ryu, D.W., Ha, S., Yoo, J.Y., Lee, K.S., 2021. Cardiac sympathetic burden reflects Parkinson disease burden, regardless of high or low orthostatic blood pressure changes. *npj Parkinson's Dis.* 7. <https://doi.org/10.1038/s41531-021-00217-3>.
- Zhang, J., Peterson, S.M., Weber, G.J., Zhu, X., Zheng, W., Freeman, J.L., 2011. Decreased axonal density and altered expression profiles of axonal guidance genes underlying lead (Pb) neurodevelopmental toxicity at early embryonic stages in the zebrafish. *Neurotoxicol. Teratol.* 33, 715–720. <https://doi.org/10.1016/j.ntt.2011.07.010>.
- Zhu, H.L., Meng, S.R., Fan, J.B., Chen, J., Liang, Y., 2011. Fibrillization of human Tau is accelerated by exposure to lead via interaction with His-330 and His-362. *PLoS One* 6. <https://doi.org/10.1371/journal.pone.0025020>.